

## Original Article

**Cite this article:** Bumby A, Grantham GH, and Moabi NG (2020) The structural evolution of the Straumnsnutane and western Sverdrupfjella areas, western Dronning Maud Land, Antarctica: implications for the amalgamation of Gondwana. *Geological Magazine* **157**: 1428–1450. <https://doi.org/10.1017/S0016756819001523>

Received: 7 May 2019

Revised: 11 December 2019

Accepted: 15 December 2019

First published online: 10 February 2020

**Keywords:**


Gondwana amalgamation; Kuunga Orogeny; deformation history; western Dronning Maud Land

**Author for correspondence:**

Geoffrey Grantham,

Email: [ghgrantham@uj.ac.za](mailto:ghgrantham@uj.ac.za)

# The structural evolution of the Straumnsnutane and western Sverdrupfjella areas, western Dronning Maud Land, Antarctica: implications for the amalgamation of Gondwana

Adam Bumby<sup>1</sup>, Geoffrey H. Grantham<sup>2</sup>  and Neo Geogracious Moabi<sup>3</sup>

<sup>1</sup>Department of Geology, University of Pretoria, Hillcrest, Pretoria, South Africa; <sup>2</sup>Department of Geology, University of Johannesburg, PO Box 524, Auckland Park 2006, South Africa and <sup>3</sup>Council for Geoscience, P/Bag X112, Pretoria, 0001, South Africa

**Abstract**

The study area is located across the Kalahari Craton – Maud Belt boundary in Dronning Maud Land (DML), Antarctica. The ~1100 Ma Maud Belt in the east is situated where the ~900–600 Ma East African and ~530–500 Ma Kuunga orogenies overlap. The Kalahari Craton cover in the west of the study area comprises ~1100 Ma Straumnsnutane Formation lavas in Straumnsnutane. In Straumnsnutane, early ~1100 Ma low-grade structures suggest top-to-the-NW deformation. Younger ~525 Ma structures suggest conjugate top-to-ESE and -WNW transport under low-grade conditions. Western Straumnsnutane and Ahlmannryggen do not show the same complex deformation, the intense deformation being restricted to NE Straumnsnutane along the eastern margin of the Kalahari Craton. In Sverdrupfjella, in the east, the Maud Belt is underlain by medium-grade, deformed ~1140 Ma supracrustal gneisses and younger intrusions. Four deformation phases in the gneisses comprise  $D_1 + D_2$  with top-to-the-N and -NW folds,  $D_3$  top-to-the-S and -SE folding and  $D_4$  brittle faulting. Syn- $D_3$  emplacement of granitoid veins is inferred at ~490 Ma. Comparison of the deformation vergence of NE Straumnsnutane with western Sverdrupfjella suggests  $D_1$  in Straumnsnutane is correlatable with  $D_1 + D_2$  Mesoproterozoic structures in western Sverdrupfjella.  $D_2$  deformation in Straumnsnutane can be correlated with  $D_3$  structures and Cambrian-age granites in Sverdrupfjella.  $D_2$  deformation in eastern Straumnsnutane and  $D_3$  in western Sverdrupfjella are inferred to have occurred in a mega-nappe footwall, implying the Ritscherflya Supergroup cratonic cover in eastern Straumnsnutane was partially submerged in the footwall, the mega-nappe formed during Gondwana amalgamation, involving collision between N and S Gondwana in the Kuunga Orogeny, ~530–500 Ma ago.

**1. Introduction**

Western Dronning Maud Land (WDML) is strategically located in an area where the inferred extents of the East African Orogeny (EAO) and the Kuunga Orogenies (KO) overlap (Figs 1, 2). The processes and timing of these orogenies are inferred to have contributed to the amalgamation of Gondwana, and consequently an understanding of the nature of deformation in the study area (Fig. 2) can contribute to an insight into the interpreted configurations and timing of Gondwana amalgamation.

**1.a. East African Orogeny**

The EAO was originally proposed by Stern (1994, 2002) to extend from the Arabian–Nubian shield to northern Mozambique and was inferred to involve a Wilson cycle from *c.* 900 Ma to *c.* 600 Ma in which East Gondwana collided with West Gondwana with the opening and closure of the Mozambique Ocean. Jacobs *et al.* (1998) proposed a geographical extension to the EAO, to central Dronning Maud Land (CDML), Antarctica, and a geochronological extension to include *c.* 500 Ma age deformation in Dronning Maud Land (DML). The age of the deformation was constrained by K–Ar and Ar–Ar dating of mica and amphibole in Heimefrontfjella (Jacobs *et al.* 1995, 1996, 1997, 1999). Jacobs *et al.* (1998, 2003a, b, c), Jacobs and Thomas (2004) and subsequent papers concluded that an intercontinental-scale transpressional sinistral shear structure for the East African Antarctic Orogen was involved in the amalgamation of East and West Gondwana, stretching from central East Africa to Heimefrontfjella (Figs 1, 2). Within the study area (Fig. 2), a suture was inferred along the west as part of the large-scale shear structure. The nature of the suture in the study area was not defined, however, but was inferred to be sinistral northwards in southern Africa and dextral to the south in Heimefrontfjella. The positioning of the sutures of the intercontinental-scale sinistral shear along the E and W was reportedly inferred from earlier publications of Grunow *et al.*

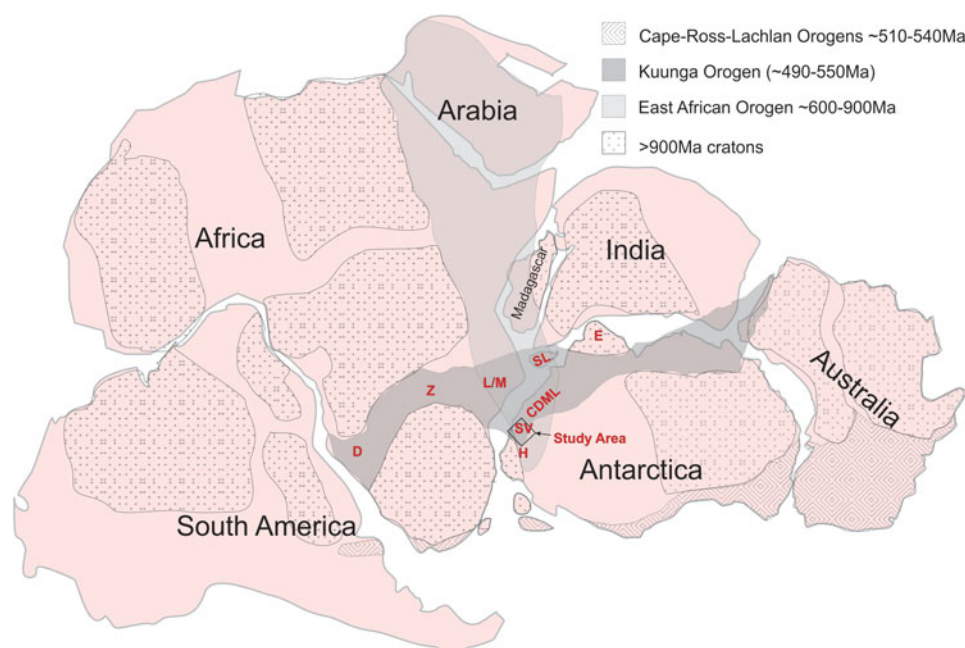


**Fig. 1.** (Colour online) Reconstruction of Gondwana showing the location of the study area in a locality within the inferred extents of the East African Orogeny and the Kuunga Orogeny. D = Damara, Namibia; Z = Zambesi, Zambia; M/L = Mozambique/Lurio belts, Mozambique; SL = Sri Lanka, E = Enderby Land, Antarctica; H = Heimefrontfjella, Antarctica.

(1996), Shackleton (1996) and Wilson *et al.* (1997). The sutures defined by Shackleton (1996) along the west comprise orthogonal W- to WNW-directed thrust fault zones toward cratonic blocks in central and southern Africa and west Dronning Maud Land (WDML) with no strike-slip component defined. Shackleton (1996) recognized top-to-the-SE thrust zones in the Lurio Belt and Sri Lanka, and Grunow *et al.* (1996) and Wilson *et al.* (1997) discuss various permutations of sutures in southern Africa and Antarctica and suggested an eastern suture linking the Lutzo-Holmbukta area with the Shackleton Range across Antarctica, separating a Pan-African Belt in the west from an Antarctic Craton in the east. Fitzsimons (2000) similarly inferred Cambrian sutures through the Sri Lanka – Lutzo Holmbukta areas and a separate one in the Shackleton range area but did not support continuity between the two areas. Mieth & Jokat (2014) conclude that there is no aeromagnetic geophysical data in support of an inferred suture linking Lutzo Holmbukta with the Shackleton Range. Fitzsimons (2000) reflects a dominant 650–550 Ma orogen across the Nampula Terrane of northern Mozambique; however, subsequent data from that area (Grantham *et al.* 2008; Bingen *et al.* 2009; Macey *et al.* 2010) have reported a dominantly Mesoproterozoic basement which has a metamorphic overprint of <570 Ma with ages >600 Ma only recorded in granulite-grade klippen (Grantham *et al.* 2013; Macey *et al.* 2013).

Structural data published from Heimefrontfjella and Gjelsvikfjella (Jacobs *et al.* 1996, 2003a), both areas in DML adjacent to the study area, contributed to the inferred EAO extension to Heimefrontfjella (Fig. 2). In Heimefrontfjella, a dextral oblique strike-slip curvilinear shear zone in the north reportedly becomes a frontal ramp with dip-slip in the south (Jacobs *et al.* 1996). Late D3 shearing of Pan-African c. 500 Ma age is inferred as having a top-to-SE sense of shear. At this locality, the dextral sense of shear is inferred to contribute to the escape southwards of a smaller crustal block (Jacobs & Thomas, 2004). Age constraints from these structures

are reported in Jacobs *et al.* (1995, 1996, 1997, 1999), with Ar–Ar ages on biotite being typically c. 500 Ma and hornblende ages c. 550–500 Ma except for the Kottas Terrane with hornblende ages of c. 1000 Ma.

In Gjelsvikfjella, at the western end of CDML (Fig. 2), Jacobs *et al.* (2003b) recognized two events, with an early dilational event at c. 558 Ma and a later event between 530 and 490 Ma with limited associated deformation. Whereas the association with deformation with these events was reported, the deformation trajectory directions were not reported. Significantly, a WNW–ESE-oriented thrust fault with top-to-the-S and -SSW stretching lineations was described; however, no strike-slip sinistral deformation was reported. Baba *et al.* (2015) report a shear zone with location and orientation in Gjelsvikfjella similar to that of Jacobs *et al.* (2003b), and describe granulites in the hanging wall with ages between c. 598 Ma and 633 Ma, indicating that the S to SSW thrusting is younger than c. 598 Ma. Jacobs *et al.* (2003b) reported granitoid and limited basic magmatism in Gjelsvikfjella and further east in CDML and Mozambique (Jacobs *et al.* 2008), which they described as being late tectonic and related to extensional post-orogenic collapse related to delamination of the orogenic root of the EAO. The direction of inferred extension was not defined. Structural trend maps from CDML are described in Jacobs *et al.* (1998, 2003c) showing an ENE-striking shear in the Orville Shear Zone, with sinistral sense of shear inferred to be of Pan-African age (Bauer *et al.* 2003). The Orvinfjella Shearzone has been correlated with the Namama Shearzone (Cadoppi *et al.* 1987) in Mozambique (Grantham *et al.* 2003), where it terminates within the Nampula Complex and consequently does not represent a suture.

### 1.b. Kuunga Orogeny

In a detailed study of geochronological data, Meert (2003) proposed a marginally younger orogenic event (c. 570–530 Ma)

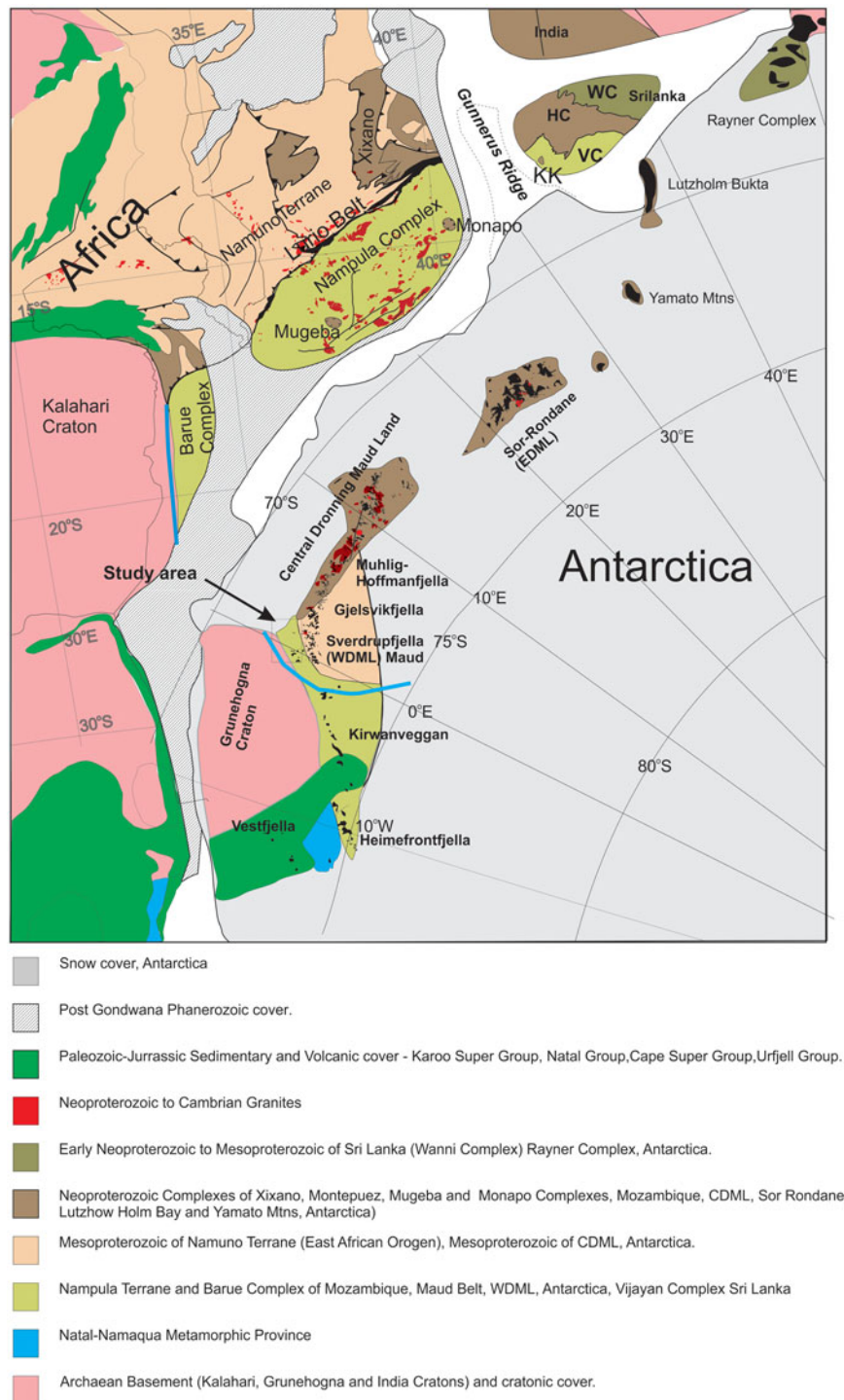


**Fig. 2.** (Colour online) Simplified geological map of a portion of reconstructed Gondwana showing correlated units between the different continental blocks. The study area location is shown along the boundary of the Kalahari Craton and Maud Belt. Abbreviations for Sri Lanka are WC = Wanni Complex, HC = Highlands Complex, VC = Vijayana Complex and KK = Kataragama Klippen. The blue line reflects the nappe extent inferred in this study.

over-printing the EAO and termed it the Kuunga Orogeny (KO) (Fig. 1). The KO was interpreted as extending from the Damara in Namibia, through the Zambesi belt, across northern Mozambique, into DML, Antarctica, through southern India and Sri Lanka, south of Enderby Land, Antarctica, and into western Australia (Fig. 1). In support of the Kuunga Orogeny, Grantham *et al.* (2008), proposed a continent–continent collision setting between N and S Gondwana, based on correlated lithological,

structural, geochronological and metamorphic  $P$ – $T$  conditions between southern Africa, DML and Sri Lanka. The collisional model proposed N Gondwana being thrust southwards over S Gondwana involving a mega-nappe structure with tectonic transport of up to *c.* 500 km between N Mozambique and DML (Figs 1, 2). Fundamental to the mega-nappe model are (a) the significance of klippen structures along the northern margin of southern Gondwana comprising the Naukluft Nappes of the

Damara Orogen in Namibia, Urungwe Klippen (N Zimbabwe), Mavhuradohna Complex (NE Zimbabwe), Mugeba and Monapo Klippen (Mozambique) and Kataragama Klippen (Sri Lanka) (Fig. 1; Grantham *et al.* 2008) and (b) the recognition that the lithologies in CDML are lithologically and geochronologically dissimilar to those of the Nampula Complex (Fig. 2) in Mozambique but similar to those of the Namuno Terrane, north of the Lurio Belt (Fig. 2) (Grantham *et al.* 2008). The locations of the latter three klippen, correlated with the Namuno Complex, are shown in Figure 2 and imply that the Nampula Complex (Mozambique) and Vijayan Complex (Sri Lanka) were in the footwall of a nappe complex, the hanging wall now largely removed by erosion. The geology of CDML was also inferred to be allochthonous, being correlatable with rocks from the Namuno Terrane of northern Mozambique (Grantham *et al.* 2008). The wider and larger extent of the CDML nappe structure was inferred to result from lower erosion rates in ice-covered Antarctica (Grantham *et al.* 2008), recognizing that the Antarctic ice sheet is inferred to have grown at least since 35 Ma (Rose *et al.* 2013), as well as loading of the continent under the Antarctic ice sheet (Grantham *et al.* 2008) given that the Antarctic ice sheet is up to 5 km thick locally. In contrast, the Nampula Complex has experienced higher rates of erosion and uplift, reflected by fission track data since Gondwana break-up *c.* 190 Ma ago, being located in a subtropical climate (Daszinnies *et al.* 2009). Grantham *et al.* (2013) described further details of lithological, geochronological and metamorphic similarities between the Monapo Klippen in Mozambique and eastern Sør Rondane in DML, in support of the mega-nappe model, and extending it onto the Antarctic continent. Grantham *et al.* (2019) broadened the longitudinal extent of the mega-nappe in the west to Gjelsvikfjella and eastern Sverdrupfjella from the original inference of CDML in Grantham *et al.* (2008) and constrained the latitudinal extent of the mega-nappe in WDML to Sverdrupfjella and N Kirwanveggan, based on new  $^{40}\text{Ar}/^{39}\text{Ar}$  age and Nd/Sr whole-rock radiogenic isotope data. The  $^{40}\text{Ar}/^{39}\text{Ar}$  cooling ages from biotite and hornblende in Sverdrupfjella and Kirwanveggan demonstrate that  $\sim$ 500 Ma metamorphism and deformation did not extend to southern Kirwanveggan and beyond to Heimefrontfjella, indicating that extension of the EAO along the eastern margin of the Kalahari Craton was invalid, given that Heimefontfjella is separated from Kirwanveggan by sedimentary basins of *c.* 550 Ma old Urfjell Group and overlying Karoo-age sedimentary rocks in Kirwanveggan (Fig. 2). Grosch *et al.* (2015) and Grantham *et al.* (2019) conclude that east Sverdrupfjella was tectonically emplaced over West Sverdrupfjella in mid- to late Pan-African times. Grantham *et al.* (2019) demonstrate that east Sverdrupfjella is isotopically distinct from west Sverdrupfjella, having juvenile protoliths with Nd depleted mantle ages (TDM)  $<c.$  1800 Ma, in contrast to western Sverdrupfjella with TDM ages  $>c.$  2000 Ma. Syntectonic granitic veins intruding both E and W Sverdrupfjella, with isotopic characteristics consistent with being sourced from the older W Sverdrupfjella basement crust, with ages of *c.* 490 Ma, show top-to-the-SE sense of shear during emplacement with extensional and compressional displacements in a simple shear setting (Grantham *et al.* 2019).

The term Maud Belt was proposed by Groenewald (1993) referring to the lithologies underlying WDML which were assumed to be Mesoproterozoic in age, based on the available data. The extent of the Maud Belt has been revised in Mendonidis *et al.* (2015) in which it is now recognized that the Maud Belt is marginally younger, at *c.* 1140 Ma, than the Natal–Namaqua Belts of southern Africa at *c.* 1225 Ma (Grantham *et al.* 2011), the boundary between

the two belts being located in Heimefrontfjella. Northwards in Gondwana, the Maud Belt, now recognized as being exposed in W Sverdrupfjella (Grantham *et al.* 2019), is correlated with the Barue Complex and its extension to the Nampula Complex in N Mozambique (Grantham *et al.* 2011) (Fig. 2). Consequently in Antarctica, the *c.* 1140 Ma Maud Belt is restricted to western Sverdrupfjella, with eastern Sverdrupfjella being correlated with the CDML domain (Grantham *et al.* 2019). Extensions of the Maud Belt are, however, inferred to extend through the Barue and Nampula complexes of N Mozambique into the Vijayan Complex in Sri Lanka (Fig. 2) (Grantham *et al.* 2008, 2011; Wai-Pan Ng *et al.* 2017).

In proposing the mega-nappe model, it was recognized that the inferred distance over which the nappe was emplaced varied significantly. Whereas the distance that the Kuunga nappe is thought to have covered between northern Mozambique and DML is *c.* 500–600 km, the emplacement distance related to the Urungwe Klippen, emplaced onto the northern Zimbabwe Craton in Zimbabwe, is significantly less and *c.*  $<100$  km (Grantham *et al.* 2008). The differential in distance between the two areas is channelled along the eastern margin of the Kalahari Craton and the Maud Belt to the east (Fig. 2), inferring a top-to-the-SE, dextral sense of shear for the hanging wall of the nappe at *c.* 530–500 Ma, east of the Kalahari Craton, with the Maud Belt of western Sverdrupfjella and its correlatives in Mozambique and Sri Lanka representing the footwall (Fig. 2).

The structural data described below, collected from the Straumnsnutane area in 2012/13, were aimed at determining whether any structures could be identified there, that could be consistent with the nappe model extending onto the Kalahari Craton. The structural data described below from Sverdrupfjella were collected during PhD studies (Grantham, unpub. PhD thesis, Univ. Natal (Pietermaritzburg), 1992), are summarized in Grantham *et al.* (1995, 2008) and were an integral component used in the formulation of the mega-nappe model in Grantham *et al.* (2008). In describing and discussing the structural evolution of the study area, there has been debate as to the extent and timing of the deformation history involving the description and identification of both Mesoproterozoic and Neoproterozoic/Cambrian (Pan-African) deformation phases, and whether these are recognized in the various areas and can be differentiated structurally and geochronologically. Consequently, in the descriptions and discussions below, the characteristics of both phases of deformation are described.

## 2. Geology of the study areas

### 2.a. Ahlmannrygen and Straumnsnutane

The geology of the study area in WDML comprises two geological terranes with a cratonic area located west of the Jutulstraumen Glacier and a medium-grade metamorphic terrane east of the glacier (Fig. 3). The cratonic terrane is underlain by the  $\sim$ 3067 Ma old Annandagstoppane Granite (Marschall *et al.* 2010) which is overlain by the Ritscherflya Supergroup (Wolmarans & Kent, 1982) comprising a volcano-sedimentary sequence intruded by basic sills of the Borgmassivet Suite. The Ritscherflya Supergroup comprises the sedimentary Ahlmannrygen Group and volcano-genic Jutulstraumen Group (Wolmarans & Kent, 1982). The Straumnsnutane Formation basaltic andesites are inferred as forming the topmost sequence of the Jutulstraumen Group, overlying the Fasettfjellet Formation (Watters, 1972; Watters *et al.* 1991).

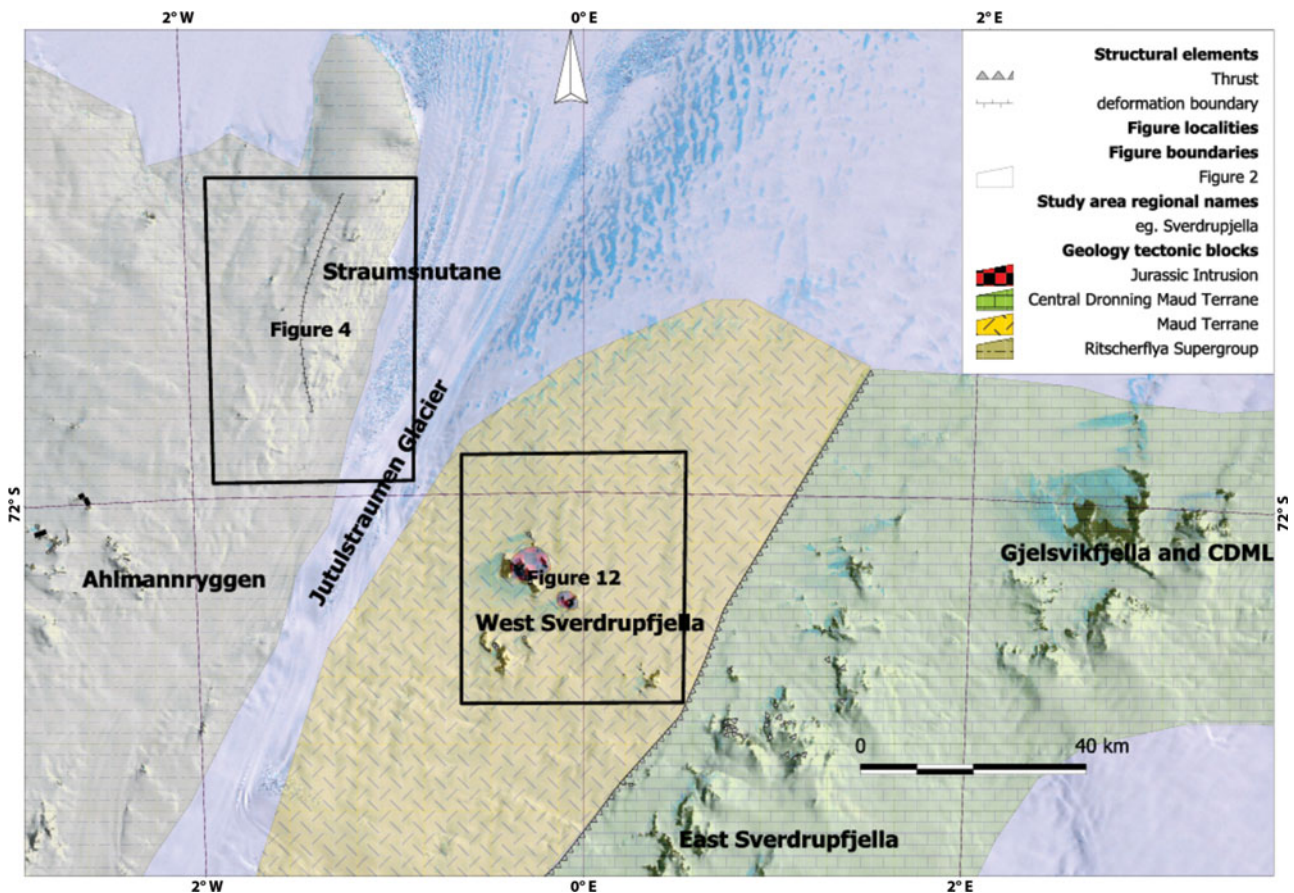


**Fig. 3.** (Colour online) Map showing the location of the study area in western Dronning Maud Land, Antarctica, spanning the Jutulstraumen Glacier, the geological provinces and localities of maps in Figure 4 and 12 in WDML. Note the inferred thrust fault boundary between east and west Sverdrupfjella (after Grosch *et al.* 2015; Grantham *et al.* 2019) separating the Maud Belt from CDML terrane.

The Straumnsnutane area of WDML (Fig. 4) is underlain by basaltic andesites and subordinate intercalated sedimentary rocks of the Straumnsnutane Formation. The age of the Straumnsnutane Formation is best constrained by the study of the detrital zircons of the sedimentary Ahlmannryggen Group, which underlies the Straumnsnutane lavas, conducted by Marschall *et al.* (2013) and by the age of Borgmassivet Suite intrusions.

Marschall *et al.* (2013) concluded that the depositional age of the Ahlmannryggen Group is  $<1125$  Ma, whereas Hanson *et al.* (2006) report an age for the Borgmassivet Suite of  $1107 \pm 2$  Ma. The data reported by Marschall *et al.* (2013) also reflect the fact that many of the zircons analysed were discordant and suggest a lower intercept age of  $\sim 550$  Ma, interpreted as resulting from low-grade metamorphism related to the 'Pan-African' amalgamation of Gondwana. Other attempts at constraining the age of the Straumnsnutane lavas using Rb/Sr methods suggested an age of  $848 \pm 28$  Ma (Eastin *et al.* 1970) with a model age of  $1664 \pm 35$  Ma. Watters *et al.* (1991) reported Sm/Nd  $T_{\text{chur}}$  model ages of between 1300 and 1620 Ma. That the model ages are significantly older than the age of  $\sim 1125$  Ma suggests that the lavas have probably been contaminated by older crust in their genesis. Peters *et al.* (1990) reported K–Ar ages of  $526 \pm 11$  Ma and  $522 \pm 11$  Ma from syntectonic white mica from a mylonite zone at Utkikken, N Straumnsnutane. Peters (1989) concluded that the white mica had grown syntectonically with K metasomatism, with the mica displaying a strong preferred planar orientation in the shear

planes. The radiogenic isotope and whole-rock major and trace element chemistry of the Straumnsnutane Formation lavas have been described by Moabi *et al.* (2017), who concluded that the chemical compositions of the Straumnsnutane basaltic andesites indicated that they are comparable to and correlatable with the Borgmassivet Intrusive Suite in WDML as well as the Espungaberra Formation basaltic andesites and Umkondo sills in southern Africa, all forming part of the  $\sim 1100$  Ma Umkondo Large Igneous Province (Hanson *et al.* 2006).

The most detailed study of the structures of the Ahlmannryggen is that of Perrit & Watkeys (2003) who concluded that gentle folding and jointing were the dominant structures. They found that the Ahlmannryggen Group showed open folding with near-horizontal fold axes, trending NE to ENE. From a detailed study of joint patterns in the Borgmassivet and Ahlmannryggen areas, they concluded that the deformation had originated from Pan-African-aged sinistral strike-slip faulting along the boundary between the cratonic Grunehogna and Maud metamorphic terranes. Watters *et al.* (1991) described intense shearing dipping  $65\text{--}70^\circ$  ESE at the eastern nunataks in Straumnsnutane, with the intensity of the shearing dissipating westwards. They reported fairly tight NE-trending folds overturned to the SE in NE Straumnsnutane. Spaeth (1987) and Spaeth & Fielitz (1987) provide the most comprehensive structural studies of Straumnsnutane to date. Spaeth (1987) described strong SE-dipping planar fabrics, as well as top-to-NW thrust faulting, referring specifically to an

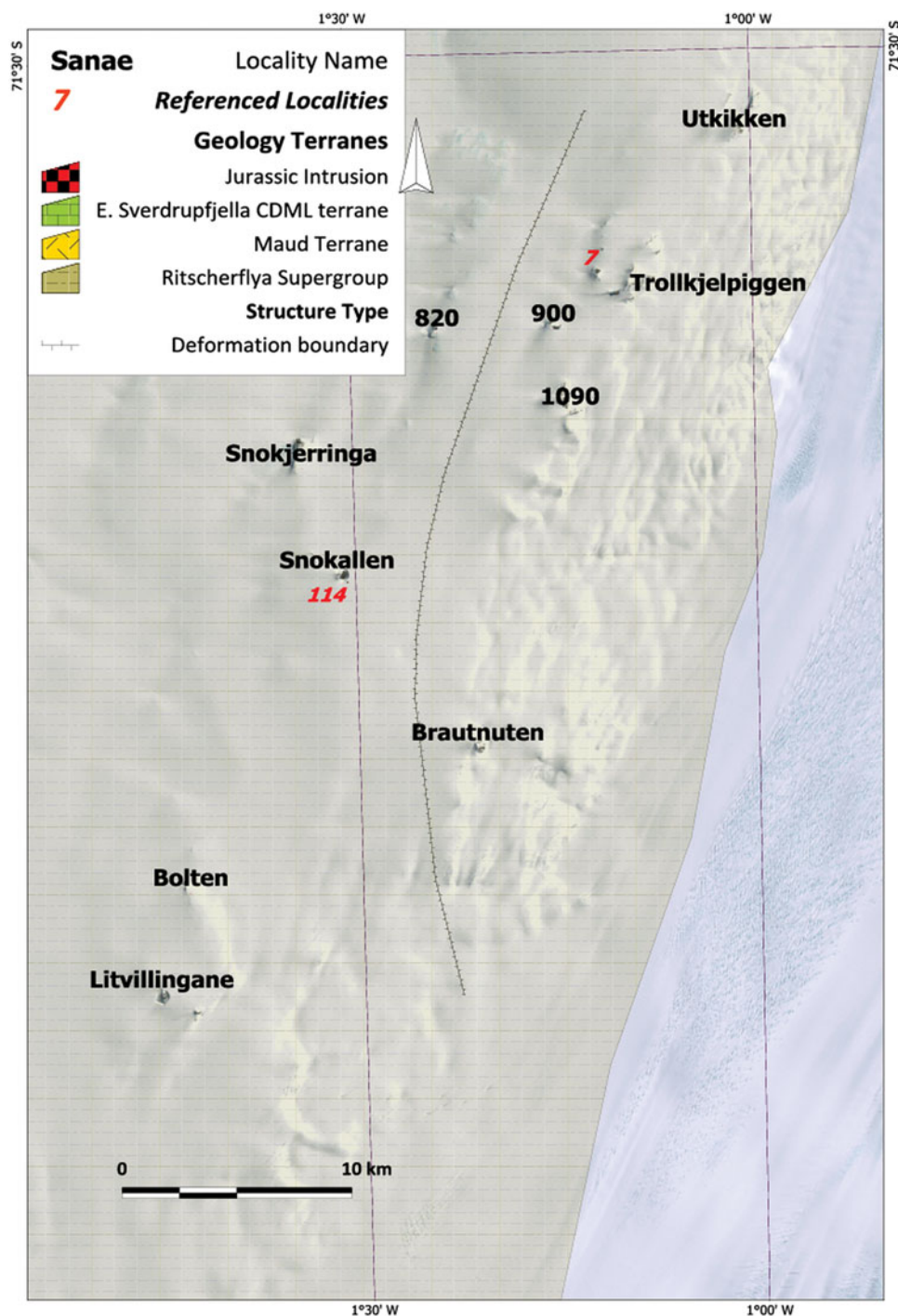


**Fig. 4.** (Colour online) Map showing the nunataks where the Straumnsnutane Formation is exposed in WDML and the names of the various nunataks mentioned as well as locality numbers described in the text. The map also shows a dividing line between strongly deformed nunataks in the east and weakly deformed nunataks in the west.

exposure (see Fig. 10 further below) at Snokallen. He also provided a description of conjugate mesoscale faulting with slickenside planes, dipping dominantly to the SE.

### 2.b. Western Sverdrupfjella

Western Sverdrupfjella is underlain by highly deformed and metamorphosed c. 1140 Ma Mesoproterozoic gneisses which have been intruded by Cambrian-age granite veins and pegmatites, meta-basic dykes of uncertain age and Jurassic alkaline complexes and

dolerite dykes. The chemistry, structural geology and metamorphic history of the gneisses and intrusions of western Sverdrupfjella have been described by Grantham (unpub. PhD thesis, Univ. Natal (Pietermaritzburg), 1992). Grantham *et al.* (2006) and Grosch *et al.* (2007) describe the chemistry and age of metamorphosed mafic dykes of varying age. Grantham *et al.* (2006) report a deformed mafic dyke, which transects migmatitic layering in tonalitic gneisses, with an upper intercept SHRIMP (sensitive high-resolution ion microprobe) U/Pb zircon age of c. 900 Ma and lower intercept age of  $523 \pm 21$  Ma. Harris *et al.* (1991),

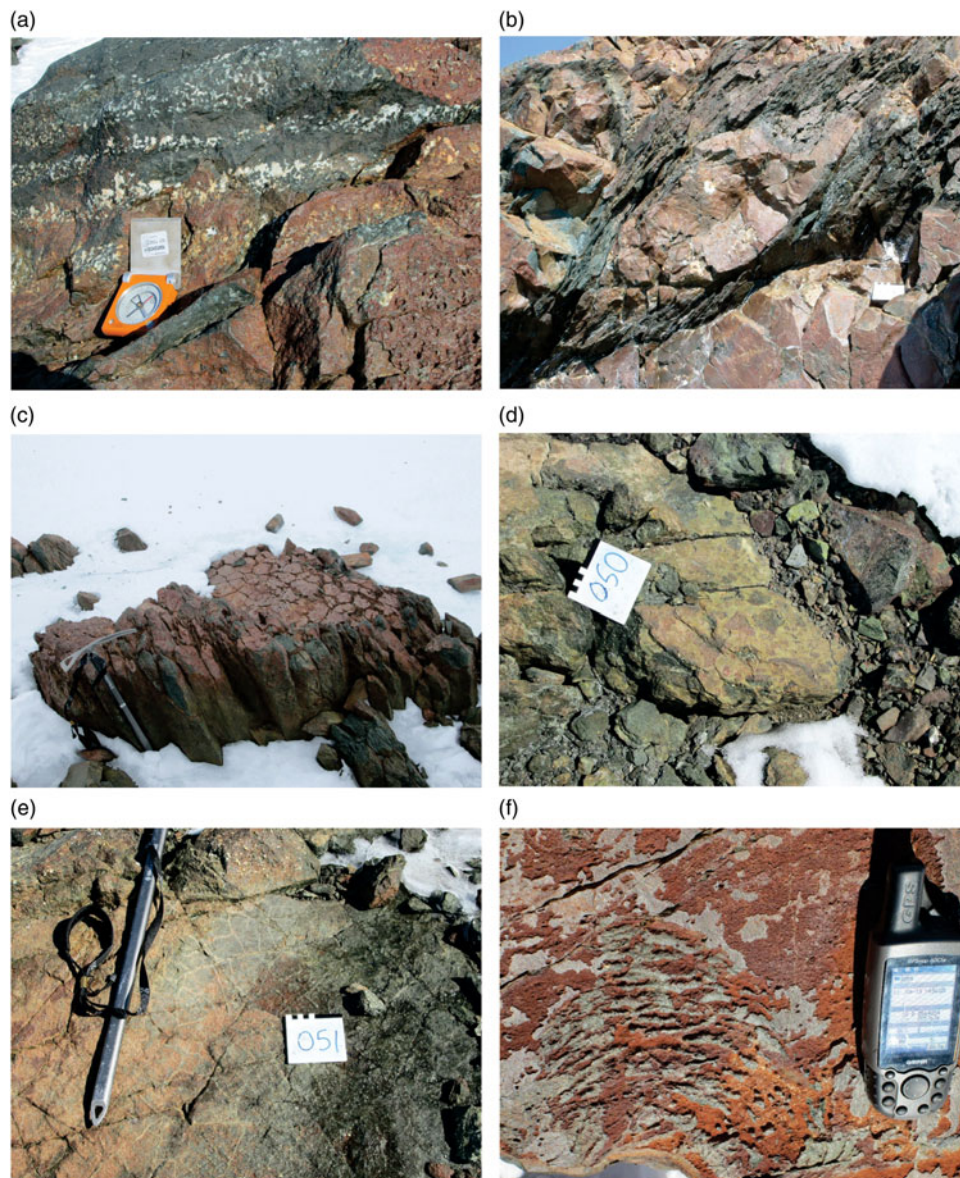


**Fig. 5.** (Colour online) Photographs of primary structures recorded in the Straumnsnutane area. Primary structures are best preserved in the western nunataks, with deformation increasing toward the Jutulstraumen Glacier in the east. (a) Layers rich and poor in amygdales. Compass for scale. (b) Flattened pillow lava. Note the strong planar fabric in the inter-pillow material and the unfoliated pillow core. The white square at lower right is 10 cm wide. (c) Partially flattened columnar jointing in basaltic andesite. Ice axe for scale. (d) Volcanic breccia fragments in basaltic andesite. The white square is 10 cm wide. (e) Cooling cracks developed in basaltic andesite. Ice axe for scale. (f) Surface pahoehoe ropy lava texture developed on basaltic andesite. GPS for scale.

Harris & Grantham (1993), Grantham (1996) and Riley *et al.* (2005) describe the geology and chemistry of Jurassic dykes and the alkaline complex at Straumsvola. Grantham *et al.* (2011) described tonalitic gneisses from western Sverdrupfjella, Kirwanveggan and northern Mozambique, with ages of *c.* 1140 Ma, in support of correlating the Maud Belt, DML, and the Barue Complex of central Mozambique. Grosch *et al.* (2015) studied the metamorphic *P–T* conditions between western Sverdrupfjella and the eastern margin of the Ahlmanryggen and concluded that the physical conditions at *c.* 500 Ma were *c.* 700 °C and 0.9 GPa and *c.* 350 °C and 0.3 GPa respectively. In addition, they concluded that western Sverdrupfjella was separated from eastern Sverdrupfjella by a thrust fault zone; however, no structural data were described in support of the conclusion. The structural history of western Sverdrupfjella has been briefly described by Grantham *et al.* (1995, 2008).

Recognizing that detailed structural studies from Straumnsnutane and Sverdrupfjella have not previously been reported, this paper is aimed at documenting and interpreting the structural geology of Straumnsnutane and western Sverdrupfjella and placing these data in a broader tectonic setting related to the amalgamation of Gondwana.

### 3. Field description

#### 3.a. Straumnsnutane

Watters *et al.* (1991) provided the most detailed description of the volcanic rocks of the Straumnsnutane Formation. They reported flow thicknesses ranging from ~1 to >50 m, with rocks being variably massive to varying degrees of amygdale development (Fig. 5a). Pillow lavas were estimated to form ~10 % of the ~850 m

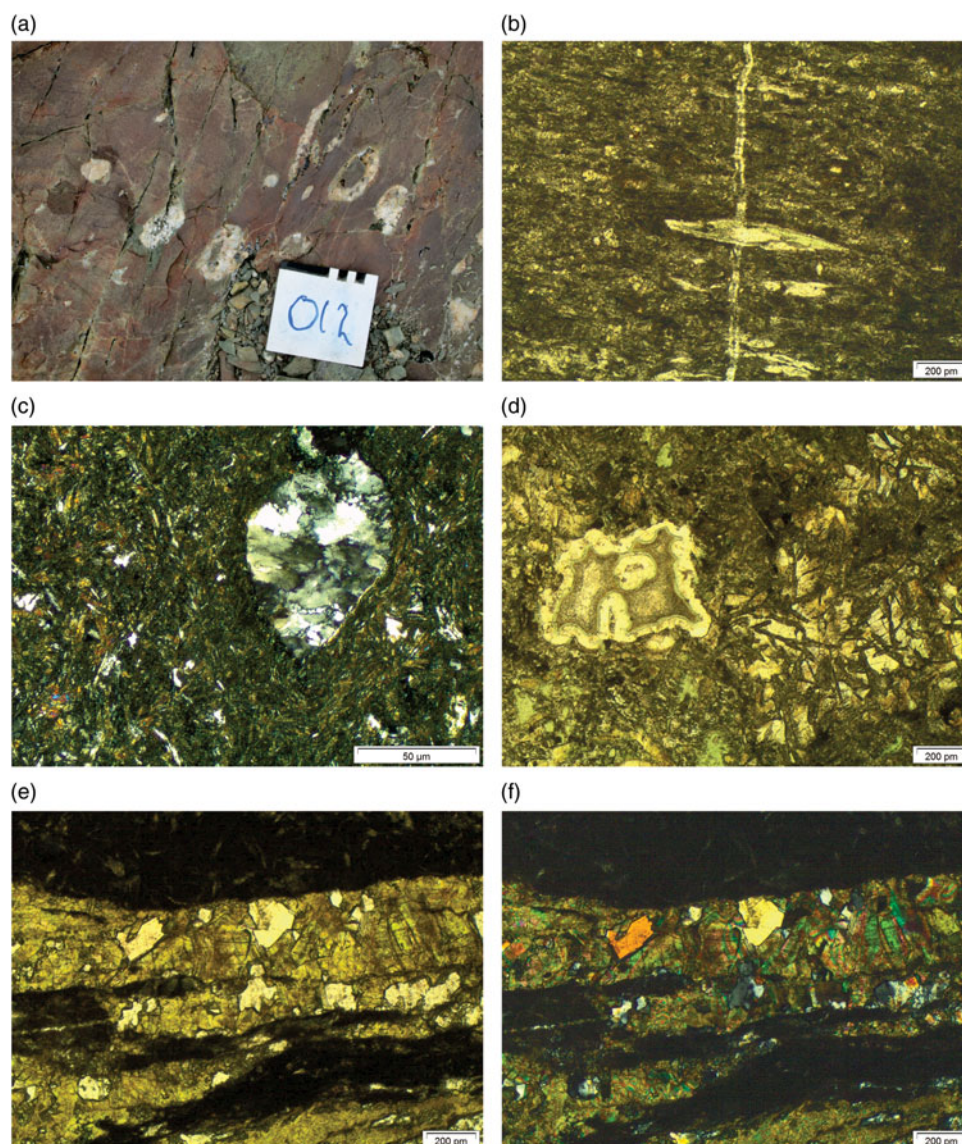


**Fig. 6.** (Colour online) Field photograph and photomicrographs of thin-sections. (a) Field photograph showing lenticular quartz tubes/blobs with cores of lavas. White square is 10 cm wide. (b) Photomicrograph of mylonitic fabric and quartz vein in sheared basaltic andesite. (c) Photomicrograph of amygdale in basaltic andesite showing strained quartz filling the amygdale. (d) Photomicrograph of zeolite-filled amygdale at left in lava with partially altered clinopyroxene at right and green chlorite at bottom centre. (e) Photomicrograph (plane polarized light) of epidote-quartz vein showing prismatic epidote. (f) Photomicrograph (crossed polars) of quartz-epidote-filled vein.

thick sequence. The pillows typically form discrete ellipsoidal bodies with shearing along the inter-pillow groundmass (Fig. 5b). At one locality deformed columnar jointing is preserved (Fig. 5c). Pillowed sequences typically grade upwards into massive lava flows (Watters *et al.* 1991). At many localities the inter-pillow areas are filled with white quartz and calcite. Thin sedimentary beds are sporadically intercalated with the lava. Nunataks along the eastern margin typically have strong planar fabrics which have destroyed primary features except amygdales. The latter are commonly elongated defining linear features typically oriented parallel to mineral and stretching lineations when developed at the same localities. Primary structures are better preserved and recognized in nunataks away from the Jutulstraumen Glacier and include volcanic breccias (Fig. 5d), cooling cracks (Fig. 5e) and ropy lava textures (Fig. 5f). At some localities large ovoid quartz lenses

are seen. The origin of these is uncertain and may be large vesicle fillings. Some of these structures have cores of lavas around which a quartz band is developed (Fig. 6a).

Primary minerals preserved in these rocks include clinopyroxene and andesine plagioclase. The rocks are extensively altered, with chlorite, white mica and epidote being common (Fig. 6d, e, f). Amygdales are filled with recrystallized quartz, zeolites and calcite (Fig. 6c, d). Serpentine pseudomorphs after olivine are seen in some samples from more basaltic compositions. Retrogressive prehnite and pumpellyite are described by Moabi *et al.* (2017). Mylonitized zones have strong planar fabrics (Fig. 6b). A detailed study of the chemistry of the lavas shows they are basaltic andesites whose genesis has probably involved mixing between a MORB (mid-ocean ridge basalt)-like basaltic magma and evolved Achaean crust at depth (Moabi *et al.* 2017).



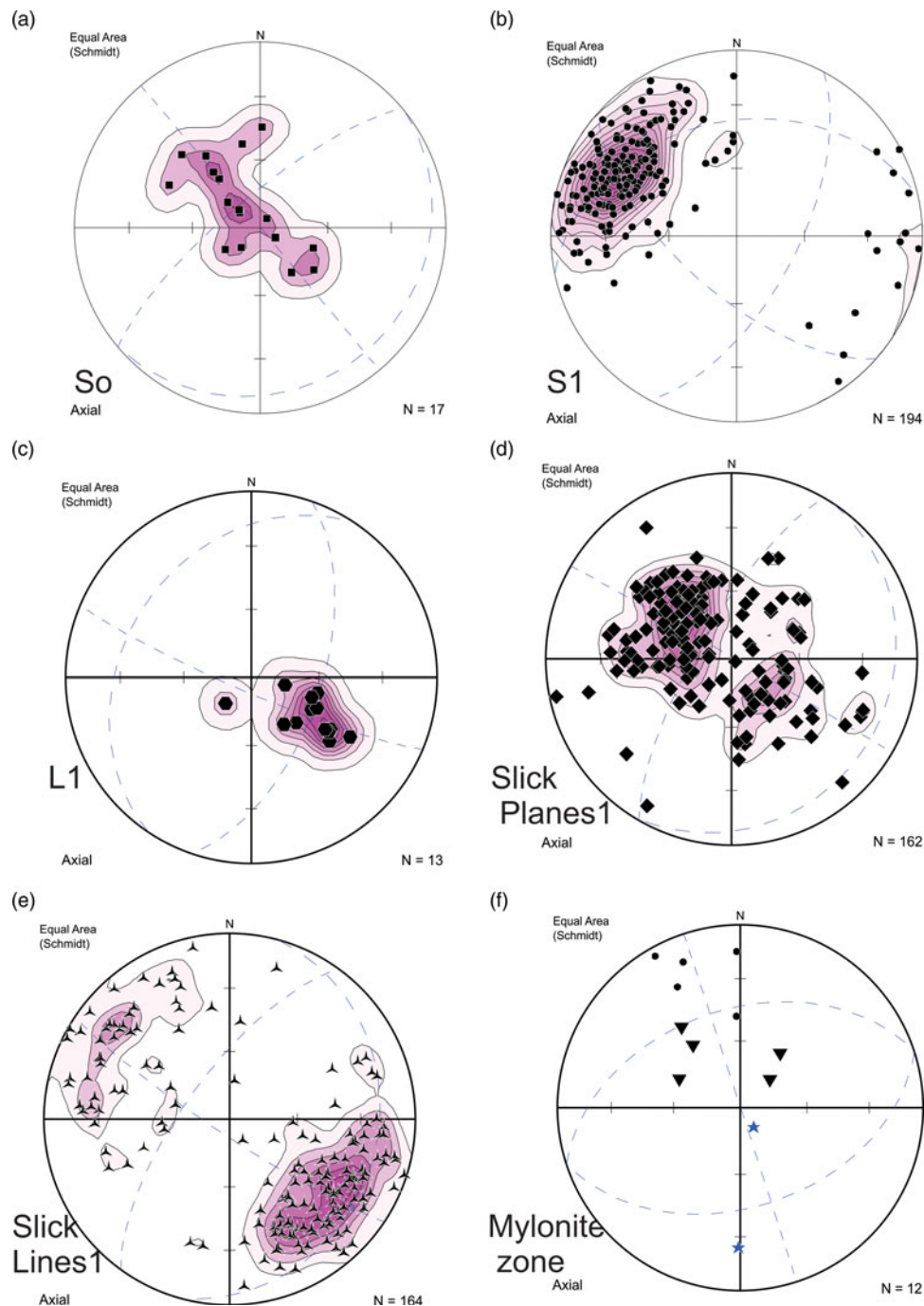


**Fig. 7.** (Colour online) Contoured stereographic projections of (a) poles to primary layering from Snokjerringa defining gentle open folding with NE/SW-oriented fold axis; (b) poles to planar  $S_1$  fabrics from the strongly sheared lavas in the west; (c) mineral and stretching lineations; (d) poles to slickensided fault surfaces; (e) lineation directions from slickensided fault surfaces; (f) structural data from the mylonite exposure described in Figure 8. Small dots are poles to planar fabrics in the country rock, inverted triangles are poles to mylonitic layering and stars are lineations in the mylonite and thrust-fault splay plane.

### 3.a.1. Structural data

Structures observed in the field can be grouped into folds, thrust faults and associated structures, small mesoscale slickensided fault planes and vein arrays. The most common structures in the field comprise planar foliations, slickensided fault surfaces with strong lineations, and quartz veins. The latter commonly form multiple generational en-echelon arrays. Less common structures include mineral and stretching lineations, and meso-scale folds.

Primary structures defining layering are rarely observed, with the clearest examples being seen at Snokjerringa, the nunatak furthest removed from the Jutulstraumen in the west (Fig. 4) and from Snokallen. Pi pole plots of primary layering, the data for which are mostly derived from Snokjerringa, define a  $\pi$  girdle oriented NW–SE (Fig. 7a), consistent with folding about a near-horizontal NE–SW-oriented fold axis. The SE-dipping layers dip shallowly to moderately ( $\sim 45\text{--}50^\circ$ ) whereas the NW-dipping layers dip shallowly, suggesting slightly asymmetric folding (Fig. 7a) and

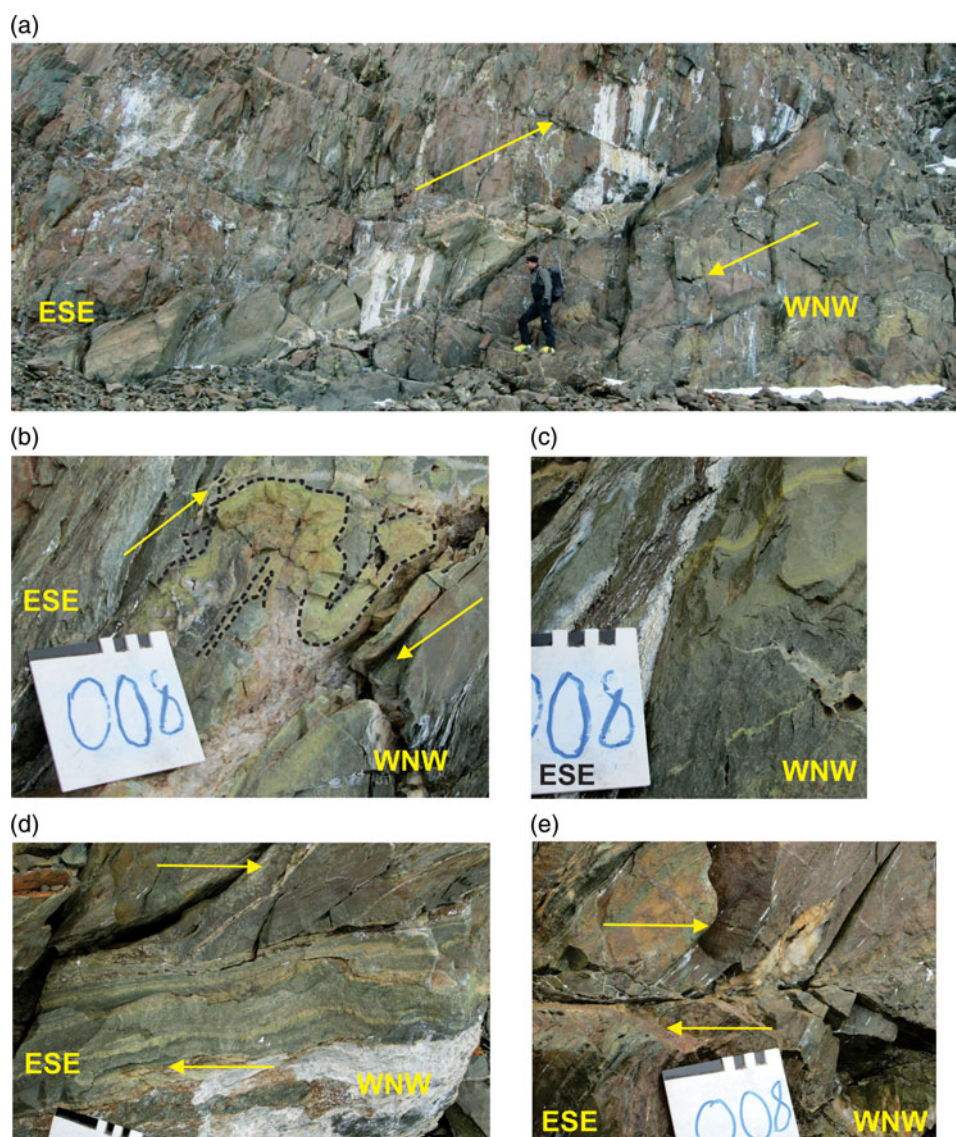


**Fig. 8.** (Colour online) Photographs of structures recorded in Straumnsnutane at locality 7 (Fig. 4). (a) View facing southwards showing a 1–2 m thick ultramylonitic layer, inclined from top right to bottom left, at SW Trollkjellpiggen. Person at lower centre for scale. The structures suggest a top-to-NW sense of shear. (b) Detailed annotated photograph showing a flow fold within the mylonitic layer defined by a pale-green epidote-rich layer showing a top-to-the-NW sense of movement. (c) Photograph of truncation of an epidote-rich layer by younger ramp structure. Note the folded quartz vein at lower right. (d) Photograph of the angular contact between the ultramylonite layer (below) and the foliated basaltic andesite above, showing a top-to-NW shear sense. (e) Photograph of a truncated quartz lens by a thrust-fault splay off the mylonite-ultramylonite layer above showing a top-to-NW shear sense.

a NW-dipping, SE-vergent axial plane. This folding has the same top-to-SE folding orientation described by Watters *et al.* (1991). In contrast, schistose planar foliations in the area are strongly developed in the east along the edge of the Jutulstraumen Glacier and are typically steep, dipping dominantly to the SE (Fig. 7b), with primary structures no longer recognizable. Sparse mineral and stretching lineations observed on the foliation planes similarly plunge steeply to the SE (Fig. 7c).

The nunatak group Trollkjellpiggen (Fig. 4) can be divided into an east and a west exposure. At the most southerly exposure of the west nunatak (locality 7, Fig. 4), a well-developed SE-dipping mylonite layer, *c.* 0.7 m thick, is exposed over *c.* 25 m before disappearing under scree rubble (Fig. 8a). Adjacent to the mylonite, the rocks have a strong planar fabric, discordant to sub-parallel to the mylonite layer (Fig. 8d), as well as several small splay offshoots (Fig. 8e). One of these splay offshoots shows clear

top-to-NW drag features with truncation of a ~10 cm ovoid quartz lens (Fig. 8e). Within the mylonite band itself, flow folds with top-to-the west geometry are defined by pale green epidote-rich layers (Fig. 8b) as well as localized truncations of internal layering (Fig. 8c). Structural data from this splay offshoot fault are presented in Figure 7f which shows steep SE-dipping planar fabrics, shallower SE-dipping mylonitic layering and steep to shallow, S-plunging lineations. Locally, the mylonite zone is truncated by folded sub-horizontal quartz veins, indicating that quartz veining post-dated the mylonitization.

In a small wind scoop, *c.* 15 m E of the mylonite band, multiple phases of quartz en-echelon vein systems are seen (Fig. 9). Four relative ages of veins can be identified from cross-cutting relationships (Fig. 9 top left and right). The oldest phase of veins is oriented near vertical and shows weak folding (Fig. 9 top left and right). In addition, the filling of the oldest vein does not show any preferred

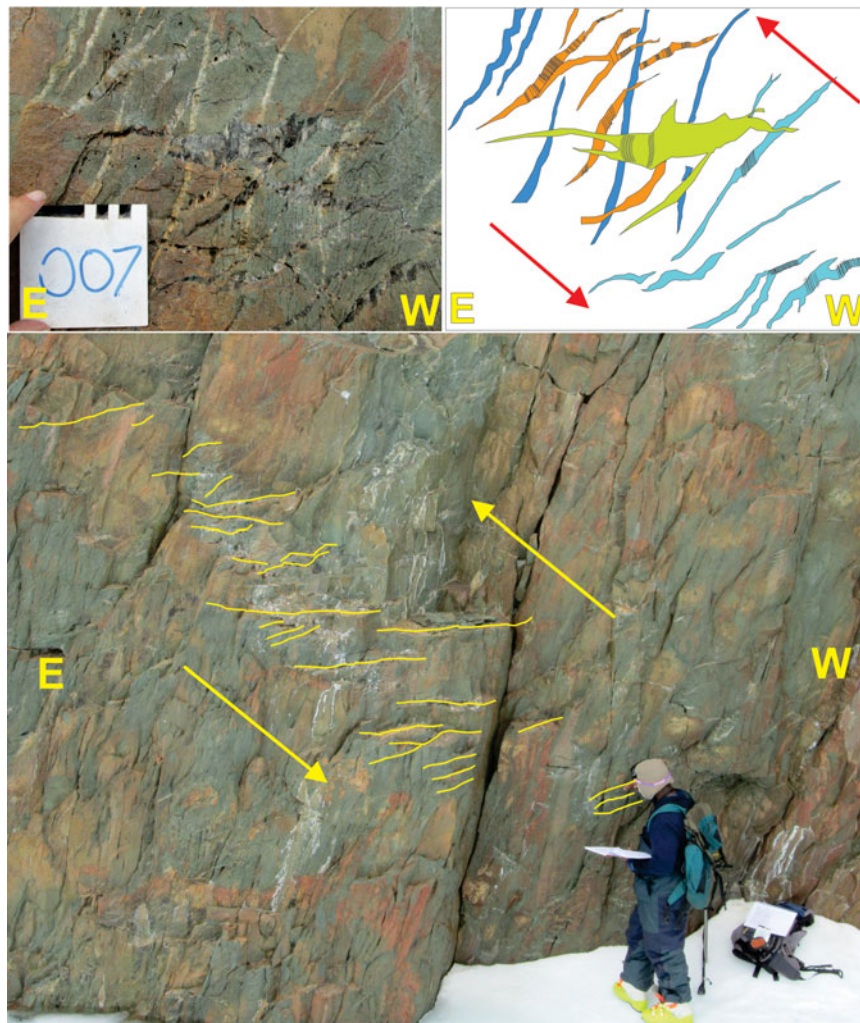


**Fig. 9.** (Colour online) Photographs of structures recorded in the Straumnutane area at locality 7 (Fig. 4). (Bottom) En-echelon quartz vein array in the edge of a wind scoop (person for scale). (Top left) Photograph showing different generations of en-echelon quartz vein generations at locality 7. The white square is 10 × 10 cm. (Top right) Sketch figure of veins at top left showing the observed veins and their relative age relationships as well as the orientation of fibrous quartz crystals within the veins shown as black lines. Blue is oldest, orange is intermediate age, green is youngest. The veins reflect an anticlockwise rotation of top-to-SE with relative age.

crystal orientation growth. In contrast, the younger vein phases show fibrous quartz growth, with the fibres mostly straight and orthogonal to vein margins, with curvilinear fibre growth being seen locally. The younger veins dip either to the east or are near-horizontal, with some of the veins being weakly sinusoidal. The vein array envelope at this locality dips westwards at  $\sim 45^\circ$  (Fig. 9 bottom). In those veins showing quartz fibre fills, the orientation of the quartz fibres is dominantly near-vertical, with minor steeply west-dipping fibres or curvilinear fibre growth (Fig. 9 top right). The dip of the vein array, with the weakly sinusoidal shapes, as well as the apparent rotation of veins from near-horizontal to near-vertical with increasing age, suggests a top-to-the-east geometry as shown in Figure 9 (Bons *et al.* 2011), with vein orientations being progressively rotated in an anticlockwise manner.

In the exposure on the southern wall of Snokallen (locality 114; Figs 4 and 10 top), a well-defined thrust fault is evident with a top-to-west geometry, similar to the structure at SW Trollkjellpiggen shown in Figure 8. This structure was previously described and similarly interpreted in a sketch by Spaeth (1987). In the exposure, it is clear that the layering of overlying sedimentary and pillowed

volcanic rocks is not disrupted by the thrust fault (Fig. 10 top), suggesting that the deformation was syndepositional. This inference would consequently constrain the top-to-the west deformation as being of Mesoproterozoic age. A large mesoscale fold with similar WNW-vergent axial plane and coarse axial planar-oriented veins (nunatak 1090; Figs 4 and 10 bottom) has a similar top-to-the-NW sense of deformation to the mylonite at Trollkjellpiggen and thrust fault at Snokallen. These large mesoscale structures suggest top-to-NW deformation during the Mesoproterozoic volcanism and sedimentation in Ahlmanryggen.

At almost all nunataks in the area, quartz-rich slickensided fault surfaces with varying attitudes and senses of movement with strong lineations are seen (Fig. 11a). Most are typically coated by pale-green amorphous epidote-rich layers and quartz. These slickensided surfaces truncate the planar fabrics at some localities, as well as the mylonite zone in Figure 8, indicating that they appear to be the youngest generation of structures in the area. Their attitudes are shown in Figure 11b, which shows WNW- and ESE-dipping slickensided fault planes, with low angles of dip generally. Hanging wall movement is almost invariably upwards or reverse, with only very few examples of oblique or strike-slip fault

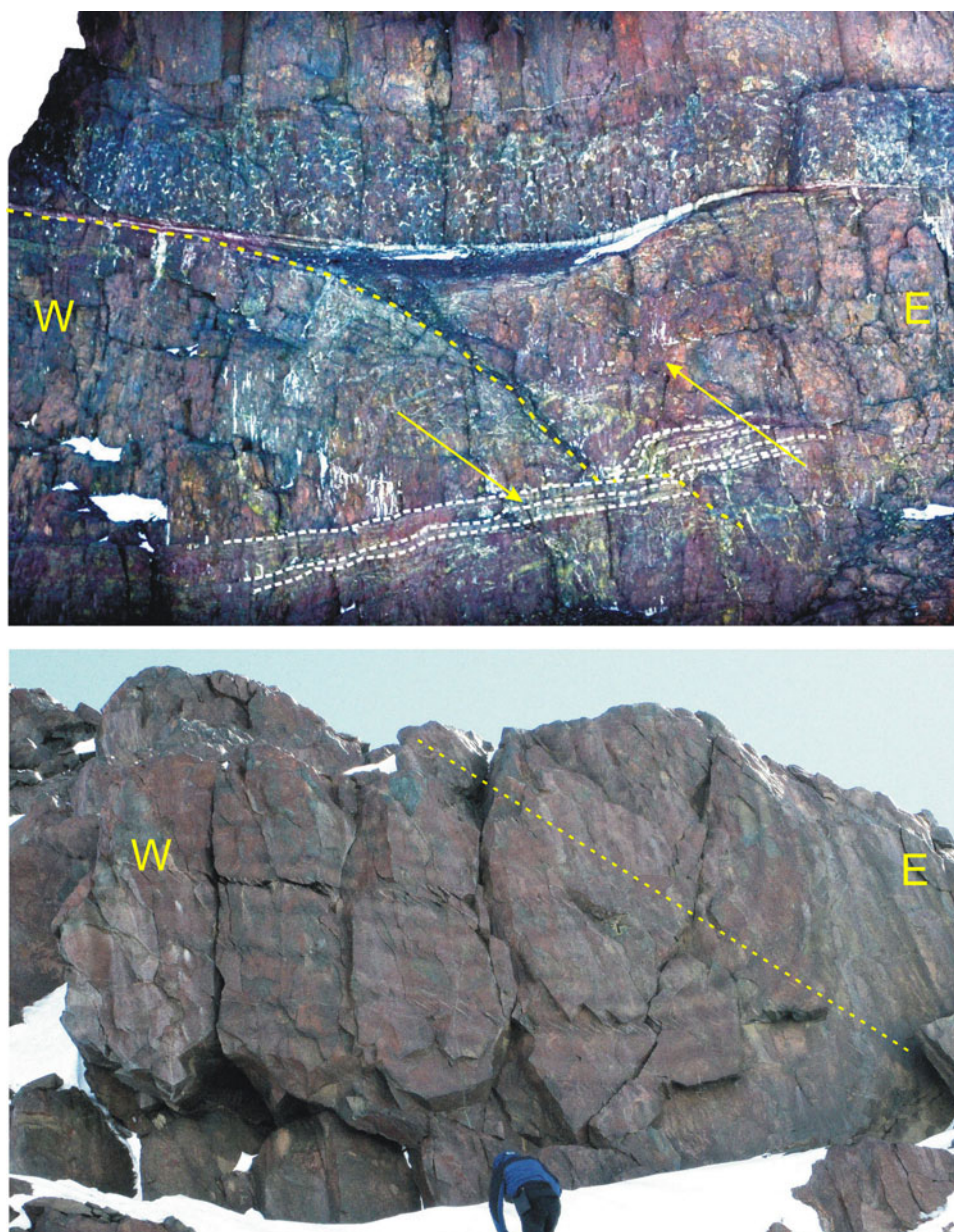


**Fig. 10.** (Colour online) Photographs of structures recorded in the Straumsnutane area at locality 114 (Fig. 4). (Above) View northwards at the southern end of Snokallen, showing a thrust fault with top-to-the-west geometry. Note the sediment and pillow-lava layers at the top of the sequence are unaffected by the faulting, suggesting that the faulting was syndepositional. This locality is similarly described and interpreted by Spaeth (1987). (Below) Photograph viewed facing north of a synclinal fold defined by layered basaltic andesite at nunatak 1090 (Fig. 4) with top-to-the-west vergence. Note the inclined axial planar fabric preferentially developed in some layers. Dashed line is an inferred axial plane.

movement. Application of the right dihedral method (Angelier & Mechler, 1977) was undertaken using Fabric 8 software for palaeostress analysis, using measurements from various individual nunataks and from the area as a whole. The data suggest that the slickensides have resulted from brittle shear with a sense of shear towards *both* the WNW and ESE (Fig. 11b–e), with  $\sigma_1$  plunging gently towards the WSW. It is possible that these relatively young structures are similar in age to the cross-cutting en-echelon quartz veins, which suggested east-vergent geometry, and thus they are inferred to have formed part of the same deformational phase, having similar senses of shear orientation, and similarly orientated palaeostress ellipsoids. Peters *et al.* (1990) reported K–Ar ages of

$526 \pm 11$ Ma and  $522 \pm 11$ Ma from syntectonic white mica from these structures.

### 3.b. Western Sverdrupfjella

Grantham *et al.* (1995) subdivided Sverdrupfjella into eastern and western areas (Figs 3, 12). Subsequent analysis of published radiogenic isotope data from the basement gneisses in Sverdrupfjella has shown that nunataks east of and including Fuglefjellet have significantly more juvenile Nd isotopic signatures ( $\epsilon\text{Nd}_{(t)}$  between  $\sim 3$  and  $-3$ ) compared to gneisses to the west ( $\epsilon\text{Nd}_{(t)}$  between  $\sim -6$  and  $-15$ ) (Grosch *et al.* 2015;

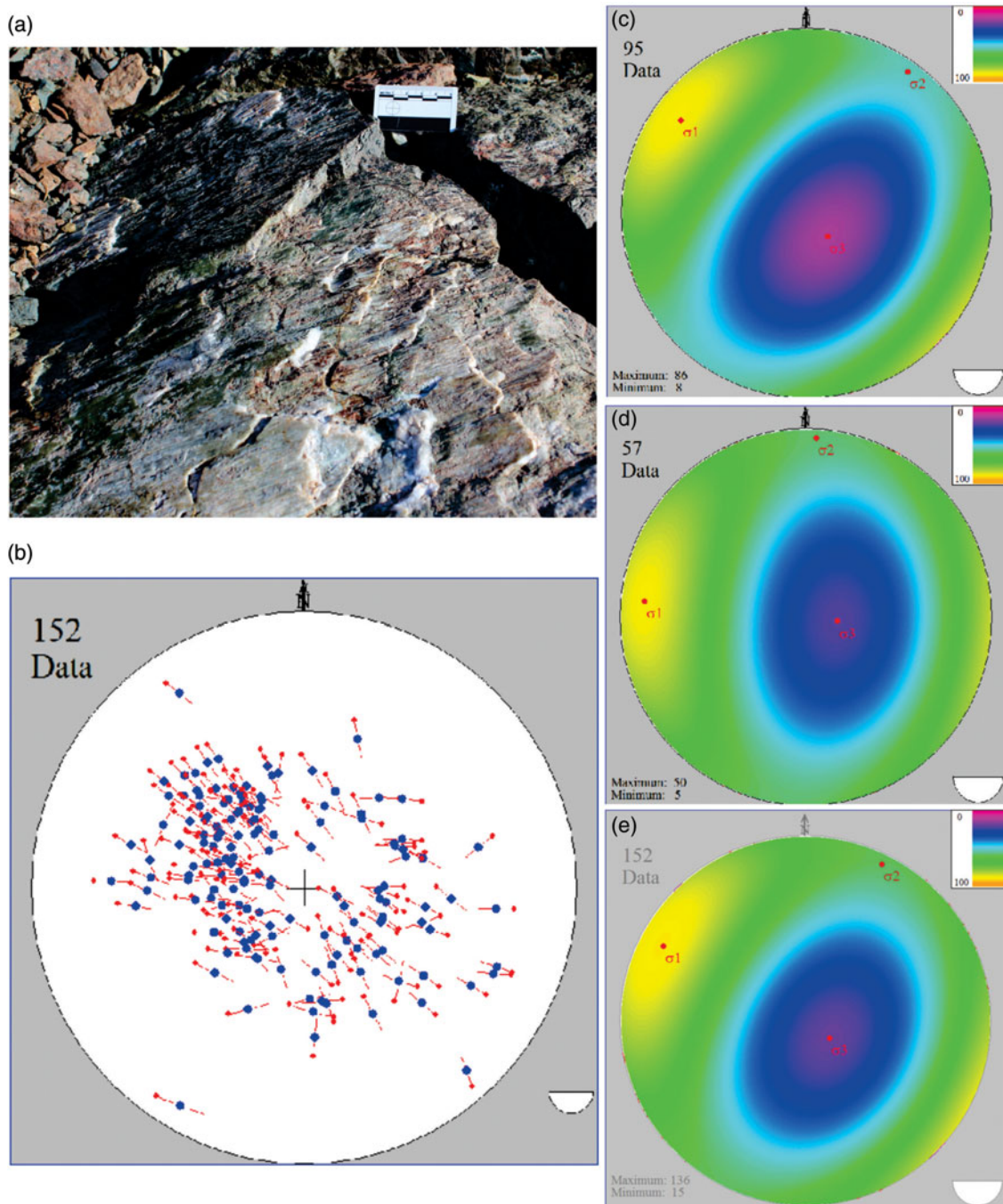


**Fig. 11.** (Colour online) (a) Photograph of an epidote-coated slickensided fault surface with strong lineations typical of many of the planes seen in Straumsnutane. (b–e) Stereographic projections summarizing the orientation of palaeostress interpreted from slickensided fault plane data using Fabric 8 software. (b) Hoenpener diagram showing orientation data from the entire area. The diagram shows poles to slickensided fault planes (blue dots) and the direction of slip of the hanging wall (red arrows). (c–e) Palaeostress reconstructions using right dihedral analysis. Cool (blue–purple) colours indicate low stress concentrations; warm (yellow) colours high stress concentrations: (c) Data from the eastern region of the study area ( $\sigma_1 = 14^\circ/327^\circ$ ;  $\sigma_2 = 12^\circ/004^\circ$ ;  $\sigma_3 = 72^\circ/116^\circ$ ). (d) Data from the western region of the study area ( $\sigma_1 = 17^\circ/294^\circ$ ;  $\sigma_2 = 12^\circ/028^\circ$ ;  $\sigma_3 = 74^\circ/140^\circ$ ). (e) Combined data from the entire Straumsnutane area ( $\sigma_1 = 20^\circ/303^\circ$ ;  $\sigma_2 = 12^\circ/038^\circ$ ;  $\sigma_3 = 72^\circ/148^\circ$ ).

Grantham *et al.* 2019). In addition, thrust faults with top-to-the-NW sense of displacement are also recognized in most nunataks east of and including Fuglefjellet (Grantham *et al.* 1995), with none recognized in west Sverdrupfjella, west of Fuglefjellet. Pressure–temperature estimates indicate that east Sverdrupfjella is characterized by isothermal decompression paths from *c.* 1.4 GPa down to *c.* 0.9 GPa (Groenewald & Hunter, 1991; Board *et al.* 2005; Pauly *et al.* 2016). In contrast,

*P–T* estimates from west Sverdrupfjella infer maximum pressures of 0.8–0.9 GPa and have a loading anticlockwise *P–T* path (Grantham, unpub. PhD thesis, Univ. Natal (Pietermaritzburg), 1992; Grantham *et al.* 1995; Grosch *et al.* 2015). Recognizing the higher pressures in east Sverdrupfjella and the general SE-dipping structural train between east and west Sverdrupfjella, an inverted *P–T* gradient is apparent, with higher pressure assemblages in east Sverdrupfjella overlying lower pressure rocks

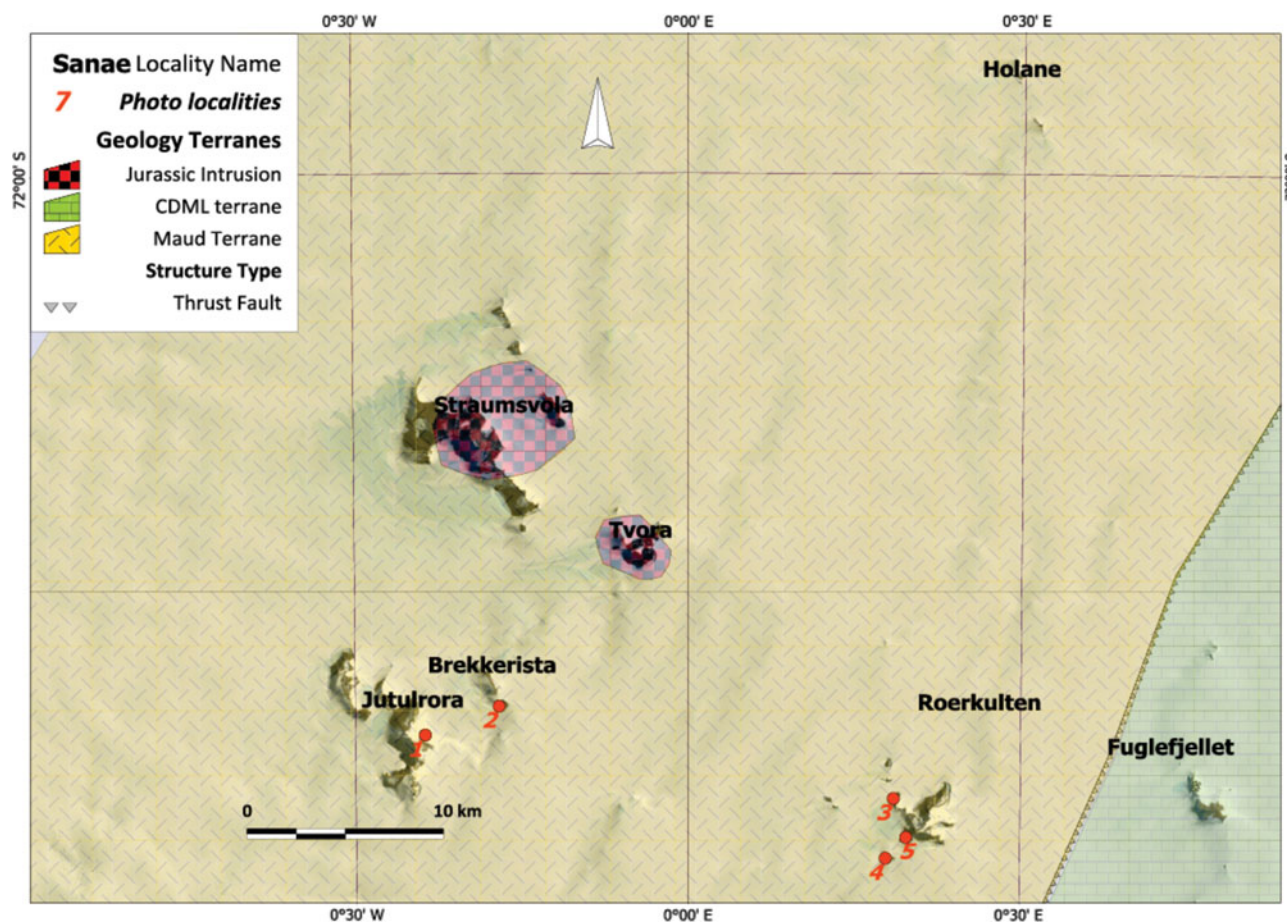


**Fig. 12.** (Colour online) Map showing western Sverdrupfjella and the names of the various nunataks mentioned in the text and localities where field photos were recorded. The location of this map in Figure 3 shows its extent in western Sverdrupfjella.

in west Sverdrupfjella. Consequently it is inferred that east Sverdrupfjella is allochthonous over west Sverdrupfjella, with the boundary between east and west Sverdrupfjella (Fig. 12) being of a tectonic, structural nature. Grosch *et al.* (2015) have also inferred east and west Sverdrupfjella being separated by a tectonic boundary, with east Sverdrupfjella being emplaced tectonically over west Sverdrupfjella. No structural data are provided by Grosch *et al.* (2015) in support of the nature of the tectonic boundary.

Western Sverdrupfjella is underlain by Mesoproterozoic supracrustal gneisses, granitic and metabasic veins and Jurassic alkaline complexes and dolerites. The supracrustal gneisses are subdivided into a Grey Gneiss Complex and Banded Gneiss Complex (Grantham *et al.* 1995), with the Grey Gneiss Complex being interpreted as being dominantly meta-andesitic in composition, typical of island-arc compositions. The Banded Gneiss Complex comprises interlayered quartzofeldspathic to metabasic gneisses, including subordinate rare calc-silicates and semi-pelitic Grt–Bt gneisses. The age and chemistry of the Grey Gneiss Complex are described in Grantham (unpub. PhD thesis, Univ. Natal (Pietermaritzburg), 1992) and Grantham *et al.* (1997, 2011) with a SHRIMP zircon crystallization age of ~1140 Ma and metamorphic rim overprints of ~600–514 Ma. Rocks with composition and mineralogy similar to the Grey Gneiss Complex, but not necessarily of the same age, are subordinate at Fuglefjellet and absent from nunataks east of Fuglefjellet.

### 3.b.1. Structural data

Grantham (unpub. PhD thesis, Univ. Natal (Pietermaritzburg), 1992) and Grantham *et al.* (1995) have described the structural history of Sverdrupfjella and Kirwanveggen and western Sverdrupfjella respectively, providing regional overview summaries. The data described below, from western Sverdrupfjella, are from Grantham (unpub. PhD thesis, Univ. Natal (Pietermaritzburg), 1992) and represent detailed structural measurements from individual localities which were summarized in Grantham *et al.* (1995, 2008). Four phases of deformation were reported from western Sverdrupfjella. Deformation phases D<sub>1</sub> and D<sub>2</sub> were described as comprising tight isoclinal recumbent fold phases with top-to-the-N and -NW vergences (Figs 13a, b, c, 14a). D<sub>1</sub> folds were recognized as having axial planar foliations (Fig. 13a) whereas D<sub>2</sub> folds were recognized in examples where the planar fabric developed during D<sub>1</sub> is folded about D<sub>2</sub> fold axes (Fig. 13b, c).

Open folds typical of D<sub>3</sub> are also evident in Figure 13b–e. D<sub>3</sub> folds were described mostly as open asymmetric, synformal folds with top-to-the-S or -SE vergences (Fig. 14 a–g) with N- to NW-dipping axial planes and near-horizontal E- to NE-plunging fold axes (Figs 14a–g, 15a–f). In Figure 14c, f, g, the exposures are intruded by thin (up to 10 m thick) SE-dipping granitic veins of Dalmatian Granite and pegmatite (Grantham *et al.* 1991) which are typically orientated at high angles or perpendicular to the axial planes of these folds. The granite veins are dilational structures whose pole orientation can be inferred to parallel the

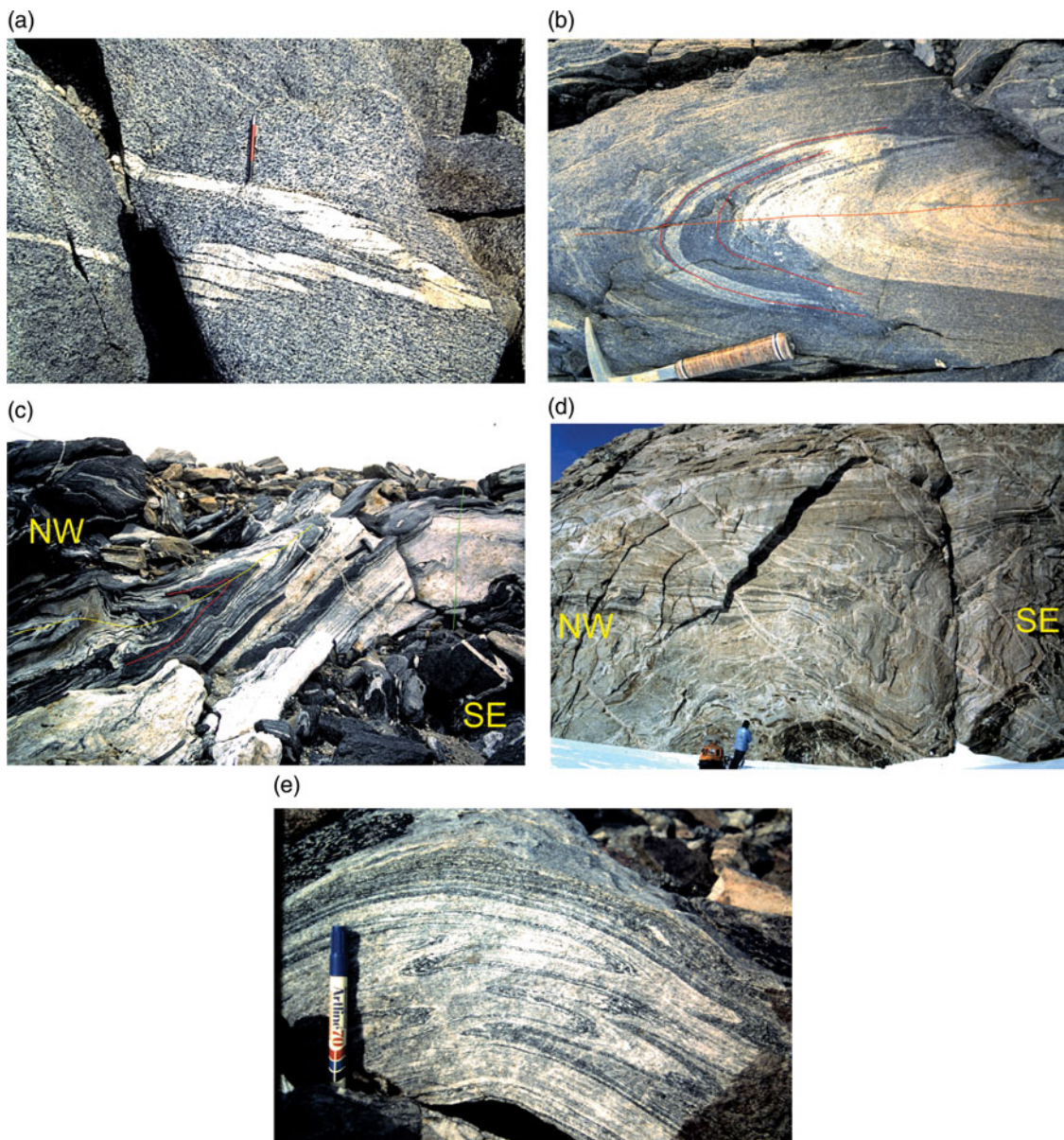


**Fig. 13.** (Colour online) Field exposures of structures at various localities in western Sverdrupfjella. (a) Near-recumbent tight  $F_1$  fold defined by a migmatitic vein in hbl-bt-qtz-feldspar gneiss. Note the axial planar foliation. (b) Tight recumbent isoclinal  $F_2$  fold, refolding an  $F_1$  fold defining a Type 3 interference fold pattern after Ramsay (1967, p. 531). Axial traces of the  $F_1$  and  $F_2$  folds are shown in red, as well as the  $F_2$  axial plane in yellow. (c) A tight isoclinal  $F_1$  fold at centre left (axial plane in red) refolded by a similarly oriented  $F_2$  fold (axial plane in yellow) in which the whole structural train is refolded around a  $F_3$  fold with ~vertical axial plane at right (green). The height of exposure is c. 2 m. (d) Partially exposed  $F_3$  upright antiformal fold at bottom centre defined by a mafic vein at Roerkulten (locality 5 in Fig. 12). Note the SE-dipping granitic veins and the strong  $F_2$  NW-vergent folding above the mafic vein. Person for scale. (e) Tight recumbent isoclinal  $F_2$  folds in finely banded gneiss refolded over a  $F_3$  open fold.

$\sigma_3$  axis of strain, prevalent during their intrusion. This orientation/relationship is also observed in Figure 14e where a metabasic layer is boudinaged/segmented, with the individual blocks separated by pegmatitic veins whose dilation direction is perpendicular to the axial plane of the  $F_3$  fold. The vergences of the folds in Figure 14a–g permit the inference of a top-to-the-south and -SE tectonic movement.

Figure 15 summarizes measurements of folds from various localities in western Sverdrupfjella. Figure 15a represents measurements of the fold shown in Figure 14c, d; it shows a c. N–S  $\pi$  girdle defined by  $S_0 + S_1$  planar fabrics and defines a shallow plunging fold axis toward ENE. The axial plane dips steeply N. Figure 15b represents measurements from the large fold

shown in Figure 14f; it shows a c. N–S  $\pi$  girdle defined by  $S_0 + S_1$  planar fabrics and defines a near-horizontal fold axis plunging toward E. The axial plane dips at c. 45° toward N. Figure 15c represents the measurements from the large fold shown in Figure 14g at Roerkulten and shows a c. N–S  $\pi$  girdle defined by the granite contact and  $S_1$  planar fabrics which define a shallow plunging fold axis toward W. The axial plane dips steeply N. Figure 15d shows measurements from the fold shown in Figure 14e. The layering  $S_0 + S_1$  dips dominantly N with axial planes dipping at c. 45° toward N and an almost horizontal fold axis plunging E. Figure 15e, f shows measurements from the fold shown in Figure 13d where an amphibolite dyke, described in Grantham *et al.* (2006), is folded. The dyke has developed a weak

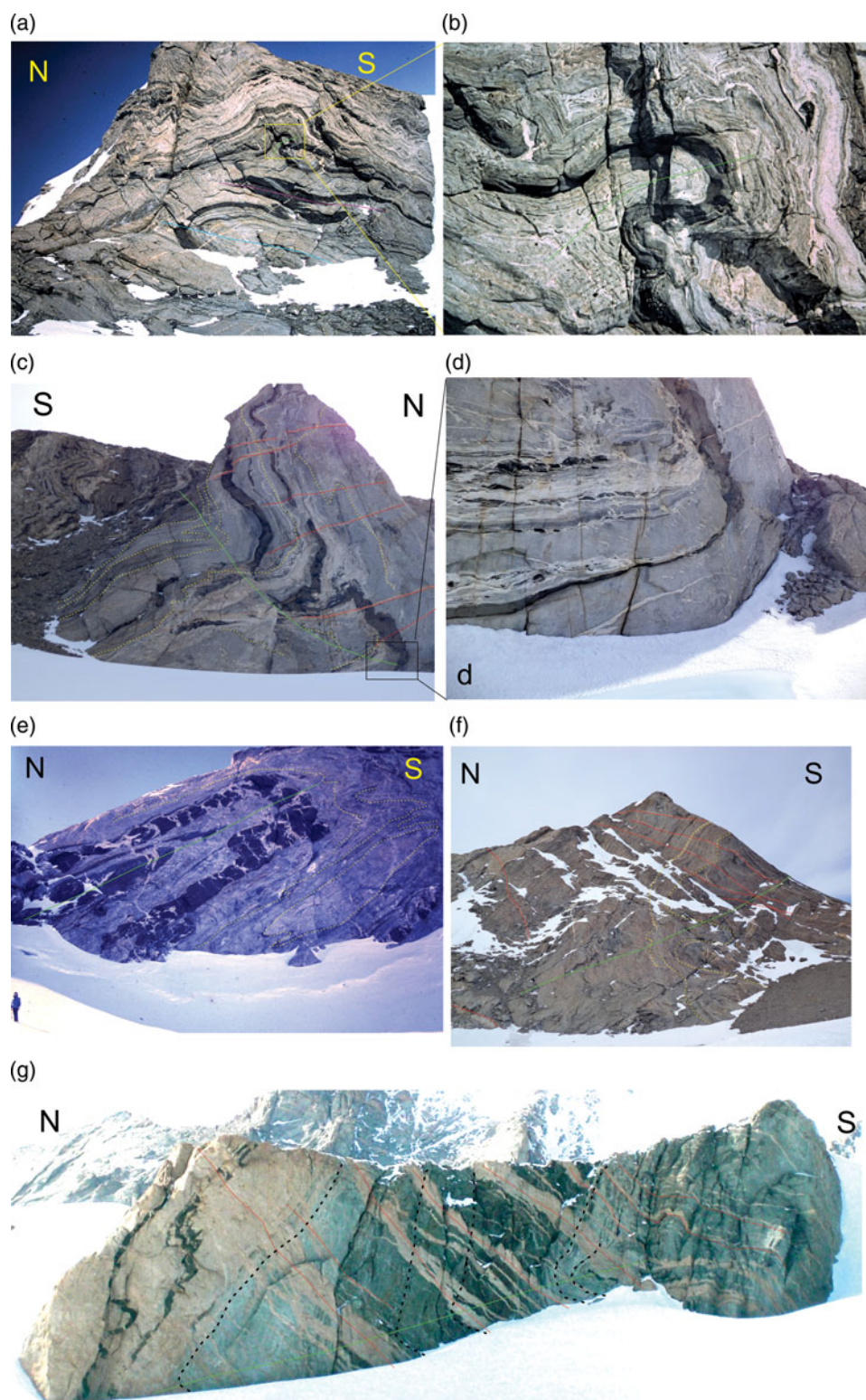


**Fig. 14.** (Colour online) Field exposures of structures at various localities in western Sverdrupfjella. (a) Exposure at Jutulrora (Fig. 12) showing the relative orientations of axial planes for  $F_1$  (purple line),  $F_2$  (blue line) and  $F_3$  folds (green line). (b) An enlargement of the axial plane of the  $F_3$  fold in (a). Height of exposure is c. 200 m. (c) Asymmetric synformal fold with S-to-SE vergence at Jutulrora (photo locality 1 in Fig. 12) Structural data from this locality are shown in Figure 15a. Note the N-dipping axial plane and the S-dipping Dalmatian Granite veins as red lines showing dilation ~perpendicular to the axial plane. (d) Enlarged insert of the fold hinge zone in the box area of (c). Note the axial planar lenticular leucosomes. (e) S-vergent isoclinal inclined fold at Roerkulten (photo locality 4 in Fig. 12). Note the dilation vein orientation of the inter-mafic boudins oriented perpendicular to the axial plane. Fold data from this locality are shown in Figure 15d. (f) Asymmetric synformal fold with southward vergence at Brekkerista (photo locality 2 in Fig. 12). Axial planar trace is shown in green. South-dipping granitic veins are shown in red. Fold data from this locality are shown in Figure 15b. (g) Asymmetric recumbent fold with S-to-SE vergence at Roerkulten and shallow NW-dipping axial plane. Cliff height is c. 100 m. Structural data from this locality are shown in Figure 15c, and the locality is photo locality 2 in Figure 12. Note the SE-dipping pegmatitic veins shown in red, and the axial planar trace shown in green, with the fold closure just above the snow line lower left.



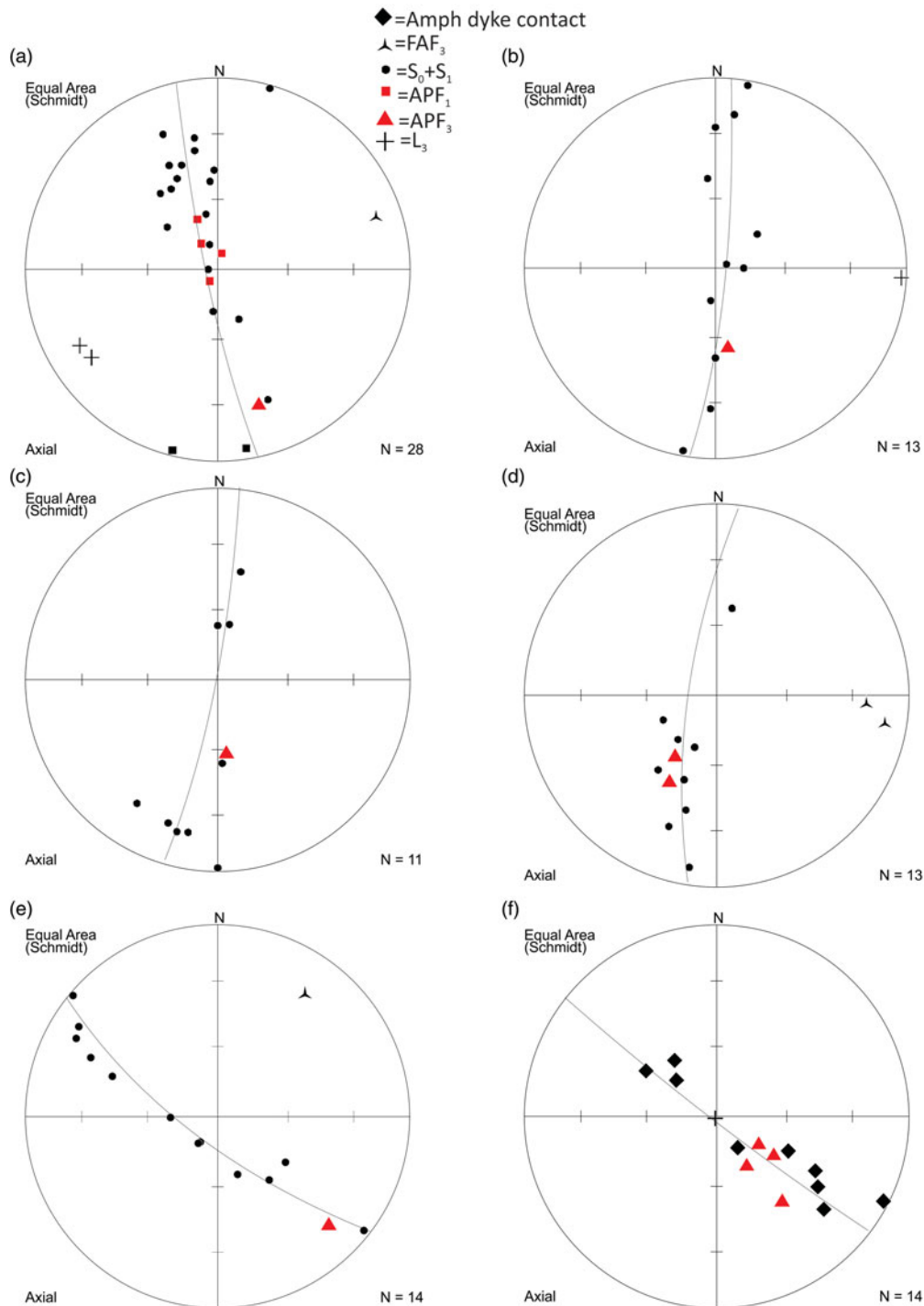


**Fig. 15.** (Colour online) Stereographic projections summarizing structural data from various localities. Abbreviations are FAF<sub>2</sub> = Fold axis F2, S<sub>0</sub> + S<sub>1</sub> = primary and F1 planar fabrics, APF1 = axial plane F1 fold, APF2 = axial plane F2 fold, L3 = lineation D3. (a) Structural data from Jutulrora (photo locality in Fig. 13) and Figure 14c, d. (b) Structural data from Brekkerista (photo locality in Fig. 12) and field photo Figure 14f. (c) Structural data from Roerkulten photo locality in Figure 12 and field photo Figure 14g. (d) Structural data from fold at Roerkulten photo locality 4 in Figure 12 and field photo Figure 14e. (e) Structural data from Roerkulten photo locality 5 in Figure 12. The data represent planar fabrics in gneiss, with the red triangle a measured NW-dipping axial plane. (f) Structural data from Roerkulten photo locality 5 in Figure 12. The black diamond data represent the contact of an intrusive amphibolite dyke, and the red triangles represent NW-dipping measured axial planar foliations in the amphibolite.

axial planar fabric which dips *c.* 45° NW. The dyke and planar fabrics in the country rock define a NW-oriented  $\pi$  girdle with near-horizontal NE-oriented fold axes. Common to all the structural measurements of the D3 folds described here in Figures 14 and 15, are folds with N- to NW-dipping axial planes, consistent

with top-to-the S and -SE transport, cross-cut by SE-dipping dilational granite sheets.

In east Sverdrupfjella, structures associated with the Dalmatian Granite veins have similarly been interpreted to represent the syntectonic emplacement of the granite with a top-to-the-SE sense

of shear (Grantham *et al.* 1991, 2019). These structures include mesoscale brittle reverse faults displacing granite vein margins but not affecting the vein intrusions, as well as extensional structures displacing earlier vein intrusions along the plane of intrusion of the granite sheets (G Byrnes, unpub. MSc thesis, Univ. Cape Town, 2015; Grantham *et al.* 2019). The displacements of the country rock layering similarly reflect a top-to-the SE deformation. Grantham *et al.* (1991) reported a Rb/Sr whole-rock – mineral isochron of  $469 \pm 10$  Ma for the Dalmatian Granite. This age is supported by a SHRIMP U/Pb zircon age of  $489 \pm 5$  Ma by Krynauw & Jackson (1996).

#### 4. Discussion and interpretation

From the structures observed in Straumnsnutane and their relative ages it can be interpreted that early top-to-NW thrust faults, folds with a horizontal, NE-trending fold axis, and strong SE-dipping axial planar foliations, represent the oldest structures in Straumnsnutane, i.e. D<sub>1</sub>. The inference that some of these structures were syndepositional in Straumnsnutane would constrain the age of this deformation to *c.* <1125 Ma, as indicated by the depositional age of the underlying Ahlmannrygen Group reported by Marschall *et al.* (2013) and the age of the Borgmassivet suite of 1107 Ma (Hanson *et al.* 2006).

Steeply SE-dipping foliation surfaces (S<sub>1</sub>), NW-vergent thrusts with well-developed mylonites, and steeply SE-plunging stretching lineations suggest a D<sub>1</sub> palaeostress ellipsoid with a gently NW-plunging  $\sigma_1$ , horizontal NE-trending  $\sigma_2$  and steeply SE-plunging  $\sigma_3$ . Such a stress ellipsoid is similar to that suggested by the D<sub>2</sub> structures (Fig. 11; see below). However, the differences in vergence, between the interpreted D<sub>1</sub> structures (NW) and D<sub>2</sub> structures (WNW, ESE and E), and difference in the style of deformation (ductile D<sub>1</sub>, exemplified by foliation and mylonitization, cross-cut by brittle/semi-brittle D<sub>2</sub>, exemplified by slickensided fault surfaces and sigmoidal en-echelon vein arrays respectively), suggests the deformation recorded in the Straumnsnutane area occurred in two separate events with D<sub>1</sub> top-to-NW and D<sub>2</sub> generally top-to-ESE.

Age constraints on the younger top-to-ESE structures (D<sub>2</sub>) are provided by the K–Ar ages on syntectonic white mica of ~525 Ma (Peters, 1989; Peters *et al.* 1990) from fault zones in Straumnsnutane which were inferred to represent the age of shearing in late-epidote–quartz-filled fault planes (Fig. 11a). Support for this age of the timing of the younger deformation is provided by the broad lower intercept ‘age’ of 600–480 Ma shown by discordant zircons reported by Marschall *et al.* (2013) which were interpreted to result from low-grade metamorphism recorded in the rocks.

The *c.* 1100 Ma-age top-to-NW D<sub>1</sub> deformation interpreted for Straumnsnutane can be correlated with the D<sub>1–2</sub> deformation described by Grantham *et al.* (1995) for the gneisses exposed in west Sverdrupfjella, where meta-granodioritic rocks with crystallization ages of ~1140 Ma (Grantham *et al.* 2011) are reported. Low U metamorphic rims on the zircon grains similarly suggest a timing of metamorphism between 514 and 660 Ma (Grantham *et al.* 2011). Early Neoproterozoic metamorphism in the Maud Province is inferred from migmatitic layering truncated by a metamorphosed mafic dyke with a poorly defined upper intercept age of ~950 Ma (Grantham *et al.* 2006).

The *c.* 525 Ma top-to-ESE D<sub>2</sub> deformation recorded for Straumnsnutane can be correlated with D<sub>3</sub> deformation described here in western Sverdrupfjella and reported by Grantham (unpub.

PhD thesis, Univ. Natal (Pietermaritzburg), 1992) and Grantham *et al.* (1995). In western Sverdrupfjella, this deformation is expressed as SE-vergent asymmetric folds at Jutulrora, Brekkerista and Roerkulten (Grantham, unpub. PhD thesis, Univ. Natal (Pietermaritzburg), 1992; Grantham *et al.* 2006) (Fig. 14a, b) with granite vein emplacement in the dilation planes of deformation. These folds have a top-to-SE vergence similar to that described by Watters *et al.* (1991) in Straumnsnutane, as well as the folding reflected in Figure 7a. The folding (Figs 13d, 15e, f) and metamorphism of a mafic dyke at Roerkulten is consistent with top-to-SE deformation and constrained by the lower intercept date of  $523 \pm 21$  Ma (Grantham *et al.* 2006). Similarly, in eastern Sverdrupfjella, the syntectonic emplacement of the Dalmatian Granite at ~470–490 Ma is consistent with a top-to-SE brittle deformation event as indicated by SHRIMP U–Pb zircon data from the Dalmatian Granite indicating a crystallization age of ~490 Ma (Grantham *et al.* 1991, 2019; Krynauw & Jackson, 1996). The age of metamorphism in western Sverdrupfjella is supported by a LA-ICPMS (laser ablation inductively coupled plasma mass spectrometer) U/Pb age from titanite from Straumsvola (Fig. 12) of  $491 \pm 27$  Ma reported by Grosch *et al.* (2015).

It is significant to note that S- to SE-vergent structures and associated SE-dipping granite sheets are limited to Sverdrupfjella and have not been reported in Kirwanveggan to the S (Grantham *et al.* 2019). Late D<sub>3</sub> shearing of Pan-African *c.* 500 Ma age is inferred as having a top-to-SE sense of shear in Heimefrontfjella; however, no syntectonic granite sheets have been recognized in Heimefrontfjella (Jacobs *et al.* 1996).

The structural characteristics for Sverdrupfjella described above and from Grantham *et al.* (1995) have contributed to the interpretation of a mega-nappe structure (Grantham *et al.* 2008, 2013, 2019) resulting from the Kuunga Orogeny in which northern Gondwana (the EAO Namuno Terrane of N Mozambique; Figs 2, 16) was emplaced over southern Gondwana between ~550 and 500 Ma, along a collision zone, between N and S Gondwana (Fig. 2b). The timing of the Kuunga Orogeny, initially inferred as being 570–530 Ma by Meert (2003), is extended to younger ages of *c.* 480 Ma, inferred from Ar–Ar data from Sverdrupfjella and Kirwanveggan (Grantham *et al.* 2019) as well as the emplacement of granite veins between *c.* 520 and 490 Ma (Grantham *et al.* 2019). An integral part of the inferred nappe structure is the top-to-SE D<sub>3</sub> folds in western Sverdrupfjella (described here) in which these folds are seen as resulting from drag compressional structures in the footwall of the mega-nappe (Fig. 16). Syntectonic emplacement of Dalmatian Granite at *c.* 490 Ma in both east and west Sverdrupfjella with top-to-SE brittle structures in east Sverdrupfjella constrains the age of the deformation. The correlation of the similarly oriented top-to-ESE D<sub>2</sub> structures in Straumnsnutane with D<sub>3</sub> structures in Sverdrupfjella consequently suggests that the nappe structure probably traversed over the eastern edge of the Grunehogna Craton in NE Straumnsnutane, as well as the Maud Belt, causing the top-to-ESE structures recorded in eastern Straumnsnutane and the west Sverdrupfjella Maud Belt. This interpretation is consistent with the low-grade metamorphic assemblages recorded in Straumnsnutane and discordant zircons reported by Marschall *et al.* (2013). Pressure–temperature estimates of ~350 °C and 0.3 GPa on a metabasite assemblage on the eastern edge of Ahlmannryggen, south of Straumnsnutane, have been reported by Grosch *et al.* (2015), implying a burial depth of *c.* 9 km, consistent with the low-grade

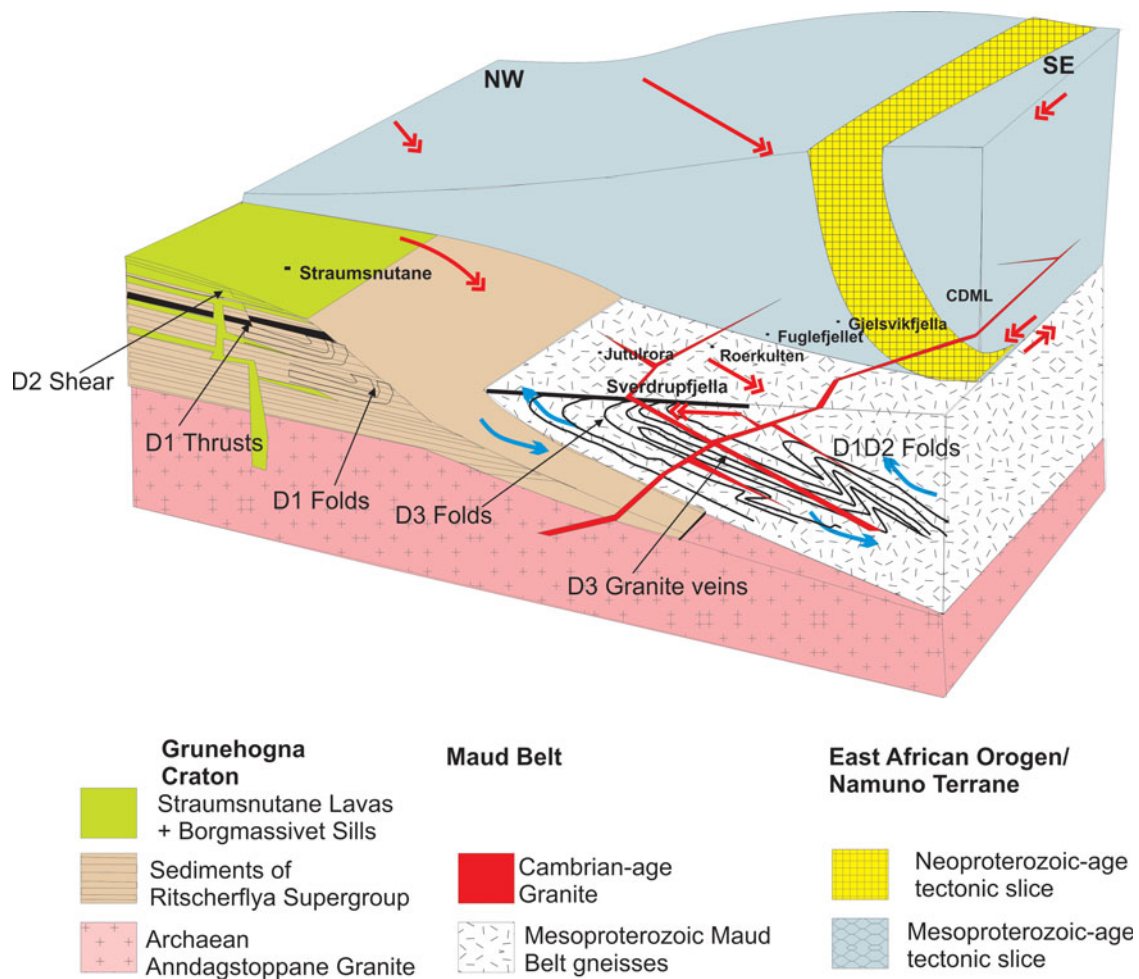


**Fig. 16.** (Colour online) Tectonic schematic interpretation of the relationships between the Grunehogna Craton, the Maud Belt and the EAO Namuno-nappe structure. Single-headed blue arrows reflect senses of shear between different blocks related to D<sub>1</sub>. Double-headed red arrows reflect inferred senses of shear between different blocks related to D<sub>2/3</sub>. The types of structures observed with inferred deformational age are shown, as well as relative schematic location in the section of geographic localities reported in the text.

minerals seen in the D<sub>2</sub> structures in Straumsnutane, and are consistent with burial and deformation beneath the nappe. No reliable thickness estimates for the Ritscherflya Supergroup in Antarctica are available, given the absence of continuous exposure in Antarctica and the difficulty of correlating sedimentary and volcanic units between nunataks. However, the Ritscherflya Supergroup is correlated with the Umkondo Group in SE Zimbabwe and central Mozambique (Hanson *et al.* 2006), which has an inferred thickness of *c.* 3.7 km (BM Bene, unpub. PhD thesis, Univ. Kwa-Zulu Natal, 2004). This would suggest that the metamorphic *P-T* estimates reported by Grosch *et al.* (2015) at *c.* 500 Ma along the margin of the Grunehogna Craton were probably the consequence of tectonic loading in the footwall, and cannot be ascribed solely to depositional burial.

In contrast, in NE Sverdrupfjella, the well-constrained *P-T* path, reflecting isothermal decompression of *c.* 1.4 GPa to *c.* 0.6 GPa from ~570 Ma to ~540 Ma from NE Sverdrupfjella (Pauly *et al.* 2016) is consistent with a continent–continent collision setting in which eastern Sverdrupfjella and Gjelsvikfjella formed a hanging-wall block with *c.* <598 Ma top-to-S and -SSW thrusting (Jacobs *et al.* 2003a, b; Baba *et al.* 2015). A doubly thickened crust in

eastern Sverdrupfjella eastwards is supported by gravity studies (Riedel *et al.* 2012) which indicate crustal thicknesses >42 km over NE Sverdrupfjella, with *P-T* studies requiring significant erosion to expose high *P-T* assemblages at current levels.

The tectonic setting envisaged is comparable to that seen currently along the western edge of the setting involving India colliding with Eurasia, contributing to the Himalayan Orogeny (Fig. 17a), with the Arabian Plate and India being subducted under Eurasia. Figure 17b shows a modified mirror image of Figure 17a, with appropriately named continental blocks inserted comprising the Kalahari Craton, Maud–Nampula Terranes (footwall) and East African Orogen – Cabo Delgado Complex – Namuno Terrane (hanging wall). The broad deformation patterns involving tectonic blocks on a similar scale in Mozambique, extending into Antarctica, are similar to those seen in the Himalayan collision zone reflected in Figure 17a. Subsequent erosion of Mozambique and, to a lesser extent, Antarctica has exposed the geology as reflected in Figure 2, in which much of the nappe inferred here and in Grantham *et al.* (2008) and Grantham *et al.* (2013, 2019) has been removed by erosion related to uplift, particularly over western Sverdrupfjella.

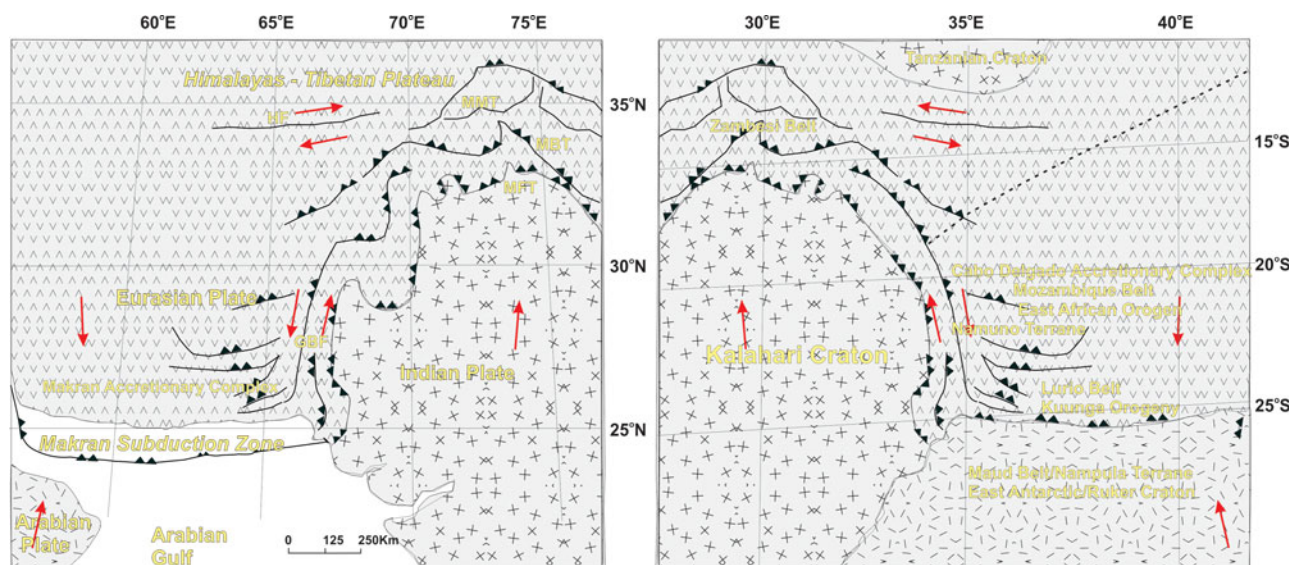


**Fig. 17.** (Colour online) (a) Plates and major structures associated with the collision between Eurasia in the north and India and Arabia in the south, with the latter plates being subducted under Eurasia. Structure names and configuration are from Crupa *et al.* (2017). MBT = Main Boundary Thrust. HF = Heart Fault. MFT = Main Frontal Thrust. MMT = Main Mantle Thrust. GBF = Ghazban Fault. (b) Modified mirror image of Figure 15a showing an inferred schematic similar configuration reflecting the Kuunga Orogeny collision between the Kalahari Craton (S Gondwana) and the Tanzanian Craton (N Gondwana) along the Damara–Zambesi–Lurio belts. The dashed line reflects the approximate present-day position of the Lurio suture under the hanging-wall block.

## 5. Conclusions

The deformation history of Straumnsnutane involved  $D_1$  top-to-the-NW thrust faulting and folding at *c.* 1100 Ma, with similarly oriented deformation of similar age being seen in W Sverdrupfjella to the east.  $D_1$  deformation in Straumnsnutane was followed by  $D_2$  deformation comprising conjugate top-to-the-ESE and -WNW deformation involving brittle semi-ductile quartz veining, SE-vergent folding and mesoscale faulting, with the timing of this deformation constrained by low-grade metamorphism at  $\sim$ 525 Ma. The deformation geometry of top-to-ESE and timing at  $\sim$ 525 Ma is similar to that recorded for  $D_3$  in Sverdrupfjella.

No evidence of sinistral displacement, consistent with a continent-scale sinistral strike-slip system, as inferred for the EAO, along the boundary between the Grunehogna Craton and the Maud Belt, interpreted by M Croaker (unpub. MSc thesis, Univ. Natal) and Perrit & Watkeys (2003), has been seen in Straumnsnutane or west Sverdrupfjella. In contrast, the  $D_2$  deformation in Straumnsnutane and  $D_3$  in Sverdrupfjella are consistent with collisional structures with southward vergence. The  $D_3$  deformation, metamorphism and intrusion of granites in Sverdrupfjella has been interpreted as resulting from the location of the area in the footwall of a south- to SE-emplaced mega-nappe structure (Grantham *et al.* 2008). The similarities in timing and style of deformation for  $D_2$  in Straumnsnutane with that of  $D_3$  in Sverdrupfjella would suggest that the nappe structure was not restricted to the Maud and CDML terranes but also partially overlapped onto and was restricted to the eastern edge of the Grunehogna Craton in Straumnsnutane, with the western Straumnsnutane, Ahlmanryggen and Borga areas showing no similar deformation. This conclusion is supported by the relatively high pressures of metamorphism along this margin, implying burial of *c.* 9 km. Late (Pan-African)  $D_3$  shearing in Heimefrontfjella similarly has a top-to-SE sense of shear (Jacobs *et al.*, 1996). Grantham *et al.* (2019) concluded that deformation along the eastern margin of the Grunehogna Craton did not affect southern Kirwanveggan and hence did not extend

to Heimefrontfjella, the oblique strike-slip shearing in Heimefrontfjella probably continuing northeastwards along the Forster Magnetic lineament to the Orvinfjella Shear zone in CDML. The deformation trajectories and related  $P$ - $T$  conditions described here for *c.* 525–480 Ma deformation in Straumnsnutane and Sverdrupfjella, and associated melting in Sverdrupfjella, as well as the published gravity data are consistent with the thickened crust mega-nappe model proposed for the Kuunga Orogeny in the WDML sector of Antarctica. On a wider scale, a top-to-S low-angle brittle shear zone with an age of  $<$ 530 Ma has been described from Sor Rondane (Tsukada *et al.* 2017) (Fig. 2). Similarly, the Kataragama Klippen in Sri Lanka is interpreted as an erosional remnant of a top-to-S (in Gondwana framework) thrust nappe (Silva *et al.* 1981) (Fig. 2) in which the Highlands Complex has been emplaced over the Vijayan Complex. This suggests the mega-nappe extended from the overlapping Kalahari Craton in the west to Sri Lanka in the east, with the Maud (W Sverdrupfjella), Barue and Nampula complexes (N Mozambique) and Vijayan Complex (Sri Lanka) representing footwall rocks to the nappe (Fig. 2).

This tectonic setting is comparable to that along the western margin of the Tibetan Plateau where India colliding northward with Asia is flanked on the west by a zone of sinistral transpressional orogeny extending through Pakistan and Afghanistan (Fig. 17a).

Within the collisional setting envisioned in Figure 16, it could be expected that dextral, top-to-the-SE displacement would occur between a footwall, comprising the Grunehogna craton plus western Sverdrupfjella, and the hanging wall of eastern Sverdrupfjella plus Gjelsvikfjella and beyond. A degree of differential shear (dextral?) could be expected between the Grunehogna craton and Maud Belt, given the thicker, more buoyant cratonic keel to the west and thinner metamorphic terrain to the east, as reflected in the gravity study of Riedel *et al.* (2012). Their study indicates crust  $>$ 42 km thick underlying the Grunehogna Craton and  $<$ 38–40 km underlying western Sverdrupfjella, increasing to  $>$ 42 km over NE Sverdrupfjella and Gjelsvikfjella eastwards.

**Acknowledgements.** Research funding provided from the NRF via a SANAP grant (80267) and a personal grant to G.H.G. (80915) is gratefully acknowledged. Logistical support from Department of Environmental Affairs is similarly acknowledged. Funding from CGS and the University of Pretoria is also most gratefully received. Constructive reviews by Horst Marschall and an anonymous reviewer are acknowledged.

**Declaration of interest.** No conflict of interest is declared by the authors.

## References

- Angelier J and Mechler P (1977) Sur une méthode graphique de recherche des contraintes principales également utilisable en tectonique et en séismologie: la méthode des dièdres droits. *Bulletin de la Société Géologique de France* 7, 1309–18.
- Baba S, Horie K, Hokada T, Owada M, Adachi T and Shiraishi K (2015) Multiple collisions in the East African–Antarctica Orogen: constraints from timing of metamorphism in the Filchnerfjella and Hochlinfjell Terranes in Central Dronning Maud Land. *The Journal of Geology* 123, 55–78.
- Bauer W, Thomas RJ and Jacobs J (2003) Proterozoic–Cambrian history of Dronning Maud Land in the context of Gondwana assembly. In *Proterozoic East Gondwana: Supercontinent Assembly and Breakup* (eds M Yoshida, BF Windley and S Dasgupta), pp. 247–65. Geological Society of London, Special Publication no. 206
- Bingen B, Jacobs J, Viola G, Henderson IHC, Skår Ø, Boyd R, Thomas RJ, Solli A, Key RM and Daudi EXF (2009) Geochronology of the Precambrian crust in the Mozambique belt in NE Mozambique, and implications for Gondwana assembly. *Precambrian Research* 170, 231–55.
- Board WS, Frimmel HE and Armstrong RA (2005) Pan-African Tectonism in the western Maud Belt: P–T–t path for high-grade gneisses in the H.U. Sverdrupfjella, East Antarctica. *Journal of Petrology* 46, 671–99.
- Bons PD, Elburg MA and Gomez-Rivas E (2011) A review of the formation of tectonic veins and their microstructures. *Journal of Structural Geology* 43, 33–62.
- Cadoppi P, Costa M and Sacchi R (1987) A cross section of the Namama Thrust belt (Mozambique). *Journal of African Earth Sciences* 6, 493–504.
- Crupa WE, Khana SD, Huang J, Khan AS and Kasib A (2017) Active tectonic deformation of the western Indian plate boundary: a case study from the Chaman Fault System. *Journal of Asian Earth Sciences* 147, 452–68.
- Daszinnies MC, Jacobs J, Wartho J-A and Grantham GH (2009) Post Pan-African thermo-tectonic evolution of the north Mozambican basement and its implication for the Gondwana rifting. Inferences from 40Ar/39Ar hornblende, biotite and titanite fission-track dating. In *Thermochronological Methods: From Palaeotemperature Constraints to Landscape Evolution Models* (eds F Lisker, B Ventura and UA Glasmacher), pp. 261–86. Geological Society of London, Special Publication no. 324.
- Eastin R, Faure G and Neethling DC (1970) The age of the Trollkjellrygg Volcanics of western Queen Maud Land. *Antarctic Journal* 5, 157–8.
- Fitzsimons ICW (2000) Grenville-age basement provinces in east Antarctica: evidence for three separate collisional orogens. *Geology* 28, 879–82.
- Grantham GH (1996) Aspects of Jurassic magmatism and faulting in western Dronning Maud Land, Antarctica: implications for Gondwana breakup. In *Weddell Sea Tectonics and Gondwana Break-up* (eds BC Storey, EC King and RA Livermore), pp. 63–71. Geological Society of London, Special Publication no. 108.
- Grantham GH, Armstrong RA and Moyes AB (2006) The age, chemistry and structure of mafic dykes at Roerkulter, H.U. Sverdrupfjella, western Dronning Maud Land, Antarctica. In *Dyke Swarms: Time Markers of Crustal Evolution* (eds E. Hanski, S Mertanen, T Ramo and J Vuollo), pp. 213–24. Proceedings of the Fifth/Fourth International Dyke Conference (IDC5), Rovaniemi, Finland. Rotterdam: A.A. Balkema Press.
- Grantham GH, Jackson C, Moyes AB, Groenewald PB, Harris PD, Ferrar G and Krynauw JR (1995) The tectonothermal evolution of the Kirwanveggen–H.U. Sverdrupfjella areas, Dronning Maud Land, Antarctica. *Precambrian Research* 75, 209–30.
- Grantham GH, Kramers J, Eglinton B and Burger EP (2019) The Ediacarian–Cambrian tectonic evolution of western Dronning Maud Land: new 40Ar–39Ar and Sr/Nd data from Sverdrupfjella and Kirwanveggen, the source of the Urjell Group and implications for the Kuunga Orogeny and Gondwana amalgamation. *Precambrian Research*. doi: 10.1016/j.precamres.2019.105444.
- Grantham GH, Maboko M and Eglinton BM (2003) A review of the evolution of the Mozambique Belt and implications for the amalgamation of Rodinia and Gondwana. In *Proterozoic East Gondwana: Supercontinent Assembly and Breakup* (eds M Yoshida, BF Windley and S Dasgupta), pp. 401–26. Geological Society of London, Special Publication no. 206.
- Grantham GH, Macey PH, Horie K, Kawakami T, Ishikawa I, Satish-Kumar M, Tsuchiya N, Graser P and Azevedo S (2013) Comparison of the metamorphic history of the Monapo Complex, northern Mozambique and Balchenfjella and Austhameren areas, Sør Rondane, Antarctica: Implications for the Kuunga Orogeny and the amalgamation of N and S. Gondwana. *Precambrian Research* 234, 85–135.
- Grantham GH, Macey PH, Ingram BA, Roberts MP, Armstrong RA, Hokada T, Shiraishi K, Jackson C, Bisnath A and Manhica V (2008) Terrane correlation between Antarctica, Mozambique & Sri Lanka; comparisons of geochronology, lithology, structure and metamorphism and possible implications for the geology of southern Africa and Antarctica. In *Geodynamic Evolution of East Antarctica: A Key to the East–West Gondwana Connection* (eds M Satish-Kumar, Y Motoyoshi, Y Osanai, Y Hiroi and K Shiraishi), pp. 91–119. Geological Society of London, Special Publication no. 308.
- Grantham GH, Manhica ADST, Armstrong RA, Kruger FJ and Loubser M (2011) New SHRIMP, Rb/Sr and Sm/Nd isotope and whole rock chemical data from central Mozambique and western Dronning Maud Land, Antarctica: implications for the nature of the eastern margin of the Kalahari Craton and the amalgamation of Gondwana. *Journal of African Earth Sciences* 59, 74–100.
- Grantham GH, Moyes AB and Hunter DR (1991) The age, petrogenesis and emplacement of the Dalmatian Granite, H.U. Sverdrupfjella, Dronning Maud Land, Antarctica. *Antarctic Science* 3, 197–204.
- Grantham GH, Storey BC, Thomas RJ, and Jacobs J (1997) The pre-breakup position of Haag Nunataks within Gondwana: possible correlatives in Natal and Dronning Maud Land. In *The Antarctic Region: Geological Evolution and processes* (ed. C.A. Ricci), pp. 13–20. Proceedings of the VII International Symposium on Antarctic Earth Sciences, Siena. Terra Antarctica.
- Groenewald PB (1993) Correlation of cratonic and orogenic provinces in southeastern Africa and Dronning Maud Land, Antarctica. In *Gondwana Eight* (eds RH Findlay, R Unrug, MR Banks and JJ Veevers), pp. 111–23. Rotterdam: Balkema Press.
- Groenewald PB and Hunter DR (1991) Granulites of northern H.U. Sverdrupfjella, western Dronning Maud Land: metamorphic history from garnet–pyroxene assemblages, coronas and hydration reactions. In *Geological Evolution of Antarctica* (eds MRA Thomson, JA Crame and JW Thomson), pp. 61–7. Cambridge: Cambridge University Press.
- Grosch EG, Bisnath A, Frimmel HE and Board WS (2007) Geochemistry and tectonic setting of mafic rocks in western Dronning Maud Land, East Antarctica: implications for the geodynamic evolution of the Proterozoic Maud Belt. *Journal of the Geological Society, London* 164, 465–75.
- Grosch EG, Frimmel HE, Abu-Alam T and Köslér J (2015) Metamorphic and age constraints on crustal reworking in the western H.U. Sverdrupfjella: implications for the evolution of western Dronning Maud Land, Antarctica. *Journal of the Geological Society of London* 172, 499–518.
- Grunow A, Hanson R and Wilson T (1996) Were aspects of Pan-African deformation linked to Iapetus opening? *Geology* 24, 1063–6.
- Hanson RE, Harmer RE, Blenkinsop TG, Bullen DS, Dalziel IWD, Gose WA, Hall RP, Kampunzu AB, Key RM, Mukwakwami J, Munyanyiwa H, Pancake JA, Seidel EK and Ward SE (2006) Mesoproterozoic intraplate magmatism in the Kalahari Craton: a review. *Journal of African Earth Sciences* 46, 141–67.
- Harris C and Grantham GH (1993) Geology and petrogenesis of the Straumsvola nepheline syenite complex, Dronning Maud Land, Antarctica. *Geological Magazine* 130, 513–32.
- Harris C, Watters BR and Groenewald PB (1991) Geochemistry of the Mesozoic regional basic dykes of western Dronning Maud Land, Antarctica. *Contributions to Mineralogy and Petrology* 107, 100–11.

- Jacobs J, Ahrendt H, Kreutzer H and Weber K (1995) K-Ar,  $^{40}\text{Ar}/^{39}\text{Ar}$  and apatite fission-track evidence for Neoproterozoic and Mesozoic basement rejuvenation events in the Heimefrontfjella and Mannefallknausane (East Antarctica). *Precambrian Research* **75**, 251–62.
- Jacobs J and Thomas RJ (2004) Himalayan-type indenter-escape tectonics model for the southern part of the late Neoproterozoic–early Paleozoic East African–Antarctic orogen. *Geology* **32**, 721–4.
- Jacobs J, Bauer W, Spaeth G, Thomas RJ and Weber K (1996) Lithology and structure of the Grenville-aged (~1.1 Ga) basement of Heimefrontfjella. *Geologische Rundschau* **85**, 800–21.
- Jacobs J, Bauer W and Fanning CM (2003a) New age constraints for Grenvillian age metamorphism in western central Dronning Maud Land (East Antarctica) and implications for the paleogeography of Kalahari in Rodinia. *Geologische Rundschau* **92**, 301–15.
- Jacobs J, Bauer W and Fanning CM (2003b) Late Neoproterozoic/Early Paleozoic events in central Dronning Maud Land and significance for the southern extension of the East African Orogen into East Antarctica. *Precambrian Research* **126**, 27–53.
- Jacobs J, Bingen B, Thomas RJ, Bauer W, Wingate MTD and Feitio P (2008) Early Palaeozoic orogenic collapse and voluminous late-tectonic magmatism in Dronning Maud Land and Mozambique: insights into the partially delaminated orogenic root of the East African–Antarctic Orogen? In *Geodynamic Evolution of East Antarctica: A Key to the East–West Gondwana Connection* (eds M Satish-Kumar, Y Motoyoshi, Y Osanai, Y Hiroi and K Shiraishi), pp. 69–90. Geological Society of London, Special Publication no. 308.
- Jacobs J, Fanning CM, Henjes-Kunst F, Olesch M and Paech HJ (1998) Continuation of the Mozambique Belt into East Antarctica: Grenville age metamorphism and Polyphase Pan-African high grade events in Central Dronning Maud Land. *Journal of Geology* **106**, 385–406.
- Jacobs J, Falter M, Weber K and Jessberger EK (1997)  $^{40}\text{Ar}/^{39}\text{Ar}$  evidence for the structural evolution of the Heimefront Shear Zone (western Dronning Maud Land), East Antarctica. In *The Antarctic Region: Geological Evolution and Processes* (ed. CA Ricci), pp. 37–44. Proceedings of the VII International Symposium on Antarctic Earth Sciences, Siena. Terra Antarctica.
- Jacobs J, Hansen BT, Henjes-Kunst F, Thomas RJ, Weber K, Bauer W, Armstrong RA and Cornell DH (1999) New age constraints on the Proterozoic/Lower Paleozoic evolution of Heimefrontfjella, East Antarctica, and its bearing on Rodinia/Gondwana correlations. *Terra Antarctica* **6**, 377–89.
- Jacobs J, Klemd R, Fanning CM, Bauer W and Colombo F (2003c) Extensional collapse of the late Neoproterozoic–early Paleozoic East African–Antarctic Orogen in Central Dronning Maud Land, East Antarctica. In *Proterozoic East Gondwana: Supercontinent Assembly and Breakup* (eds M Yoshida, BF Windley and S Dasgupta), pp. 271–87. Geological Society of London, Special Publication no. 206.
- Krynauw JR and Jackson C (1996) Geological evolution of western Dronning Maud Land within a Gondwana framework. South African National Antarctic Programme Final Report 1991–1996. Geology Subsection, 1–48.
- Macey PH, Miller JA, Rowe CD, Grantham GH, Siegfried P, Armstrong RA, Kemp J and Bacalau J (2013) Geology of the Monapo Klippe, NE Mozambique and its significance for assembly of central Gondwana. *Precambrian Research* **233**, 259–81.
- Macey PH, Thomas RJ, Grantham GH, Ingram BA, Jacobs J, Armstrong RA, Roberts MP, Bingen B, Hollick L, de Kock GS, Viola G, Bauer W, Gonzales E, Bjerkgård T, Henderson IHC, Sandstad JS, Cronwright MS, Harley S, Solli A, Nordgulen Ø, Motuza G, Daudi E and Manhiça V (2010) Mesoproterozoic geology of the Nampula Block, northern Mozambique: tracing fragments of Mesoproterozoic crust in the heart of Gondwana. *Precambrian Research* **182**, 124–48.
- Marschall HR, Hawkesworth CJ and Leat PT (2013) Mesoproterozoic subduction under the eastern edge of the Kalahari–Grunehogna Craton preceding Rodinia assembly: the Ritscherflya detrital zircon record, Ahlmannryggen, Dronning Maud Land, Antarctica. *Precambrian Research* **236**, 31–45.
- Marschall HR, Hawkesworth CJ, Storey CD, Dhuime B, Leat PT, Meyer H-P and Tamm-Buckle S (2010) The Annandagstoppane granite, East Antarctica: evidence for Archaean intracrustal recycling in the Kaapvaal–Grunehogna craton from zircon O and Hf isotopes. *Journal of Petrology* **51**, 2277–301.
- Meert J (2003) A synopsis of events related to the assembly of eastern Gondwana. *Tectonophysics* **362**, 1–40.
- Mendonidis P, Thomas RJ, Grantham GH and Armstrong RA (2015) Geochronology of emplacement and charnockite formation of the Margate Granite Suite, Natal Metamorphic Province, South Africa: implications for Natal–Maud belt correlations. *Precambrian Research* **265**, 198–202.
- Mieth M and Jokat W (2014) New aeromagnetic view of the geological fabric of southern Dronning Maud Land and Coats Land, East Antarctica. *Gondwana Research* **25**, 358–67.
- Moabi NG, Grantham GH, Roberts J and le Roux P (2017) The geology and geochemistry of the Straumnsnutane Formation, Straumnsnutane, western Dronning Maud Land, Antarctica and its tectonic setting on the western margin of the Kalahari Craton: additional evidence linking it to the Umkondo Large Igneous Province. In *Crustal Evolution of India and Antarctica: The Supercontinent Connection* (eds NC Pant and S Dasgupta), pp. 61–85. Geological Society of London, Special Publication no. 457.
- Pauly J, Marschall HR, Meyer H-P, Chatterjee N and Monteleone B (2016) Prolonged Ediacaran–Cambrian metamorphic history and short-lived high-pressure granulite facies metamorphism in the H.U. Sverdrupfjella, Dronning Maud Land (East Antarctica): evidence for continental collision during Gondwana assembly. *Journal of Petrology* **57**, 185–228.
- Perrit SH and Watkeys MK (2003) Implications of late Pan-African shearing in western Dronning Maud Land, Antarctica. In *Intraplate strike-slip deformation belts* (eds F Storti, RE Holdsworth and F Salvini), pp. 135–43. Geological Society of London, Special Publication no. 210.
- Peters M (1989) Igneous rocks in western and central Neuschwabenland, Vestfjella and Ahlmannryggen, Antarctica: petrography, geochemistry, geochronology, paleomagnetism, geotectonic implications. *Berichte zur Polarforschung* **61**, 78–80.
- Peters M, Haverkamp B, Emmermann R, Kohlen H and Weber K (1990) Paleomagnetism, K-Ar dating and geodynamic setting of igneous rocks in western and central Neuschwabenland, Antarctica. In *Geological Evolution of Antarctica* (eds MRA Thompson, JA Crame and JW Thompson), pp. 549–55. Cambridge: Cambridge University Press.
- Ramsay JG (1967) *Folding and Fracturing of Rocks*. New York: McGraw-Hill Book Co., 568 pp.
- Riedel S, Jokat W and Steinhage D (2012) Mapping tectonic provinces with airborne gravity and radar data in Dronning Maud Land, East Antarctica. *Geophysical Journal International* **189**, 414–27.
- Riley TR, Leat PT, Curtis ML, Millar IL, Duncan RA and Fazel A (2005) Early–Middle Jurassic dolerite dykes from western Dronning Maud Land (Antarctica): identifying mantle sources in the Karoo large igneous province. *Journal of Petrology* **46**, 1489–524.
- Rose KC, Ferraccioli F, Jamieson SJR, Bell RE, Corr H, Creyts T, Braaten T, Jordan TA, Fretwell PT and Damaske D (2013) Early East Antarctic Ice Sheet growth recorded in the landscape of the Gamburtsev Subglacial Mountains. *Earth and Planetary Science Letters* **375**, 1–12.
- Shackleton RM (1996) The final collision between East and West Gondwana: where is it? *Journal of African Earth Sciences* **23**, 271–87.
- Silva KPL, Wimalasena EM, Sarathchandra MJ, Munasinghe T and Dasannayake CB (1981) The geology and origin of the Kataragama Complex of Sri Lanka. *Journal of the National Science Council of Sri Lanka* **9**, 189–97.
- Spaeth G (1987) Aspects of the structural evolution and magmatism in western New Schablenland, Antarctica. In *Gondwana Six: Structure, Tectonics and Geophysics* (ed. GD McKenzie), pp. 295–307. Washington, DC: American Geophysical Union, 323 pp.
- Spaeth G and Fielitz W (1987) Structural investigations in the Precambrian of western Neuschwabenland, Antarctica. *Polarforschung* **57**, 71–92.
- Stern RJ (1994) Arc assembly and continental collision in the Neoproterozoic East African Orogen: implications for the consolidation of Gondwanaland. *Annual Reviews Earth Science* **22**, 319–51.
- Stern RJ (2002) Crustal evolution in the East African Orogen: a neodymium isotopic perspective. *Journal of African Earth Sciences* **34**, 109–17.

- Tsukada K, Yuhara M, Owada M, Shimura T, Kamei A, Kouchi Y and Yamamoto K** (2017) A low-angle brittle shear zone in the western Sør Rondane Mountains, Dronning Maud Land, East Antarctica – implication for assembly of Gondwanaland. *Journal of Geodynamics* **111**, 15–30.
- Wai-Pan Ng S, Whitehouse MJ, Tama TP, Jayasingha P, Wonga JP, Denyszyn SW, Yiu JS and Chang S-C** (2017) Ca. 820–640 Ma SIMS U-Pb age signal in the peripheral Vijayan Complex, Sri Lanka: identifying magmatic pulses in the assembly of Gondwana. *Precambrian Research* **294**, 244–56.
- Watters BR** (1972) The Straumnsnutane Volcanics, western Dronning Maud Land, Antarctica. *South African Journal of Antarctic Research* **2**, 23–31.
- Watters BR, Krynauw JR and Hunter DR** (1991) Volcanic rocks of the Proterozoic Jutulstraumen Group in western Dronning Maud Land, Antarctica. In *Geological Evolution of Antarctica* (eds MRA Thomson, JA Crame and JW Thomson), pp. 41–6. Cambridge: Cambridge University Press.
- Wilson TJ, Grunow AM and Hanson RE** (1997) Gondwana assembly: the view from southern Africa and East Gondwana. *Journal of Geodynamics* **23**, 263–8.
- Wolmarans LG and Kent LE** (1982) Geological investigations in western Dronning Maud Land, Antarctica – a synthesis. *South African Journal of Antarctic Research*, Suppl. 2, 93 pp.